MODELLING AND ANALYSIS OF A PHOTOVOLTAIC SYSTEM FOR A LOCAL BUSINESS IN WINDHOEK, NAMIBIA

A THESIS SUBMITTED IN PARTIAL FULFILLMENT OF THE REQUIREMENTS FOR THE DEGREE OF MASTER OF SCIENCE IN RENEWABLE ENERGY

OF

THE UNIVERSITY OF NAMIBIA

BY

AINA KAULUMA

201604520

OCTOBER 2024

SUPERVISOR: Dr. Petja Dobreva

Department of Physics, Chemistry and Material Science, University of Namibia

Abstract

Photovoltaic (PV) technology generates electricity from light. There are two types of PV technologies in the market: traditional monofacial solar cells, which capture light on their front side, and emergent bifacial solar cells, which capture light on both their rear and front sides. Studies focusing on the performance of bifacial solar modules in Windhoek have not yet been conducted, so their potential advantages in this location are unknown. The study aimed to model and evaluate the PV systems based on monofacial and bifacial silicon (Si) technologies. This feasability study was conducted for a business in Windhoek, Namibia. The evaluation was conducted by assessing the specific yield, performance ratio criteria, and the levelized cost of electricity (LCOE) for the systems modelled within the same specified location using the PVsyst software. The systems are a bifacial single-axis tracking PV system, a bifacial fixed-tilt PV system, a monofacial single-axis tracking PV system, and a monofacial fixed-tilt PV system, all with similar technical parameters. The results showed that the energy production of the single-axis tracking bifacial system is higher than that of the monofacial system; however, there is no statistically significant difference between the two. On the other hand, the fixed-tilt bifacial PV system significantly outperforms the fixed-tilt monofacial PV system. Additionally, the single-axis tracking monofacial PV system has the shortest payback period of 3 years, 2 months with an ROI of 35.62%, while the fixed-tilt bifacial PV system has the longest payback period of 3 years, 8 months and an IRR of 31.50%. The system that performs the best financially is the single-axis tracking monofacial PV system with an LCOE of N$ 0.85/kWh.

Contents

List of Figures

List of Tables

List of Acronyms and abbreviations

Abbreviation	Meaning
CAPEX	Capital Expenditure
CF	Capacity Factor
FF	Fill Factor
GHI	Global Horizontal Irradiation
GW	Gigawatt
Isc	Short-Circuit Current
IRR	Internal Rate of Return
I-V	Current-Voltage
Jsc	Short-Circuit Current Density
LCOE	Levelized Cost of Electricity
MPPT	Maximum Power Point Tracker
OPEX	Operational Expenditure
Pmax	Maximum Power
P&O	Perturb and Observe
PV	Photovoltaic
STC	Standard Test Conditions
TPT	Tedler Polyester Tedlar
Voc	Open-Circuit Voltage

Acknowledgments

Immense gratitude goes out to the following people whose support was instrumental in my achieving the result of this work:

- My supervisor, Dr. Petja Dobreva, for consistently and continuously providing guidance and much-needed constructive criticism that helped in developing this thesis.
- My support system, through family and friends, throughout my journey towards my master's degree. Without that foundation, I would not be where I am today.

Dedication

This thesis is a dedication to myself for continuing despite it all and to my parents for their unwavering support and words of encouragement even when I faltered. This support is one of the major reasons why I managed to accomplish completing this thesis.

Declarations

I, Aina N.I. Kauluma, declare hereby that this study is a true reflection of my own research, and that this work, or part thereof has not been submitted for a degree in any other institution of higher education.

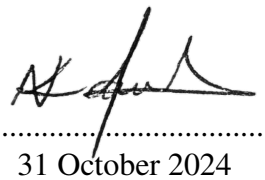

.....

31 October 2024

Chapter 1

Introduction

Photovoltaics (PV) refers to the technology which converts light directly into electricity through a phenomenon known as the photovoltaic effect [2]. When a material is exposed to light, voltage is generated, as shown in figure 1.1.

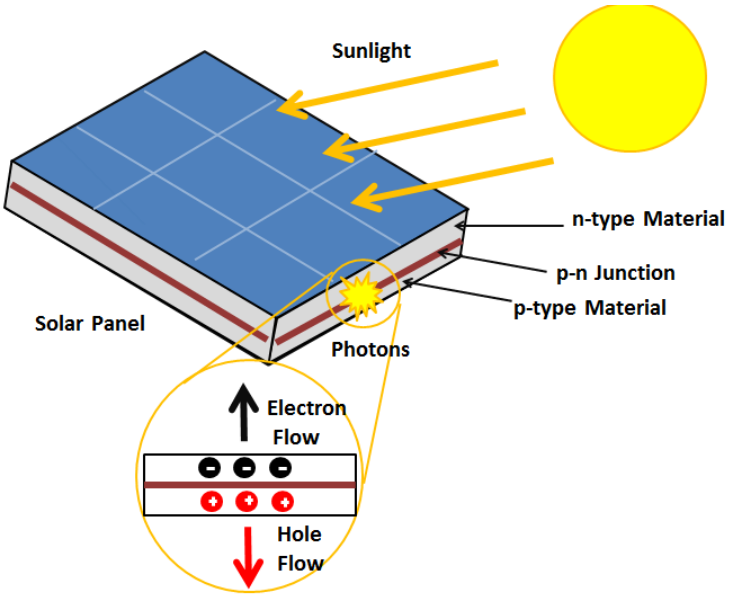

Figure 1.1: Photovoltaic Effect

Solar panels typically use monofacial solar cells that capture light on only one side. In contrast, in recent years, bifacial solar cells and modules have garnered interest for their potential to increase energy generation by capturing sunlight from both the front and back sides [3,4].

Some studies have shown that the energy output difference between monofacial and bifacial modules can be large, with an increase of up to a 30% relative increase in energy generation with bifacial modules [4]. With advancements in technology and optimisation strategies, bifacial modules are becoming more cost-effective and efficient, offering a promising alternative to traditional monofacial modules [5].

Since 2010, the price of solar panels has dropped by more than 80% [6], making it one of the least expensive sources of electricity in many regions of the world. In recent years, PV-generated electricity has become more affordable than electricity generated by conventional fossil fuels [7]. With the decline in solar panel pricing, solar PV global renewable capacity increased by 25% from 2022 to 2023 [7]. Businesses typically use PV systems in addition to or in replacement of electricity provided by the utility grid to cut down on electrical bills.

When connecting to the Namibian grid, a framework known as the Modified Single Buyer (MSB), developed by the Electricity Control Board (ECB), may be applied to commercial entities [8]. The framework states that distribution-connected customers with a demand of 1 MVA of power and above are allowed to purchase up to 30% of their energy demand from Eligible Sellers or Traders, while the remaining 70% would still be purchased from the national power utility company, Nampower [8]. Subsequently, this framework allows businesses to set up their own PV plants that can provide them with up to 30% of their load demand. Although there may be potential advantages to using bifacial modules in Windhoek's conditions, with global horizontal irradiation (GHI) levels of approximately 2332.7 kWh/m² per year [1], which have not yet been studied, additional research is necessary to enhance and validate the design and cost-effectiveness of bifacial PV systems for broader adoption. Since bifacial modules are relatively new to the Namibian market, it is crucial to prevent financial losses due to incorrect assumptions about this technology. This can be achieved through modelling and techno-economic assessments of the PV projects utilising these modules.

1.1 Problem statement

Despite the potential benefits of photovoltaic (PV) plants with bifacial modules, there is limited knowledge about their techno-economic performance in the Windhoek area. This gap in understanding poses a challenge for local businesses considering the adoption of advanced PV technologies. Without comprehensive data and analysis, businesses may struggle to make informed decisions regarding the investment and implementation of bifacial PV systems. This lack of information can hinder the optimisation of energy production and financial returns of businesses within the Windhoek area.

1.2 Objectives

The study aimed to determine whether a PV plant with bifacial modules is the most financially feasible option for a business in Windhoek to meet part of its electricity demand.

The objectives of the study were to:

(a) Develop detailed models using the PVsyst modelling software and use simulations to determine energy outputs of 3 MW tracking and fixed-tilt PV systems using novel bifacial solar modules and PV systems with monofacial solar modules in Windhoek.

(b) Assess and compare the energy performance of the photovoltaic systems using accepted performance criteria.

(c) Assess and compare the financial performance of the four PV systems.

(d) Compare the financial performance of the four PV systems to determine the feasibility of the systems for the local business entity.

1.3 Thesis Layout

In Chapter 2 the literature review serves as an analysis of the existing literature relevant to solar modules, bifacial solar modules, monofacial solar modules, fixed-tilt PV systems, and single-axis tracking PV systems incorporating these technologies.

The methodology for designing PV systems and data analysis methods deployed to analyse the data are given in Chapter 3. First, we describe the PV system design using PVsyst modelling software. In this chapter, descriptions of the financial parameters and statistical tests used to analyse the energy production of the different models is also provided.

Chapter 4 has the presentation of the results of this study.

Finally, in Chapter 5, conclusions are drawn on the basis of the results of the comparisons of the performance assessments and LCOE between the different systems. Recommendations of the most feasible system for the business are also identified within this chapter.

Chapter 2

Literature Review

2.1 Introduction

This chapter synthesizes existing research on photovoltaic (PV) technologies, emphasizing structural and operational differences between monofacial and bifacial systems. Key themes include rear-side irradiance mechanisms, performance metrics such as specific yield and levelized cost of electricity (LCOE), and environmental factors like albedo and temperature. The analysis is grounded in Namibia's exceptional solar resource potential, where global horizontal irradiation (GHI) averages 2,118-2,500 kWh/m²/year (Fig. 2.1) [1], creating an ideal environment for PV adoption. By contextualising global insights on bifacial performance within Namibia's arid climate and high albedo, this review identifies critical gaps in localized data for bifacial systems.

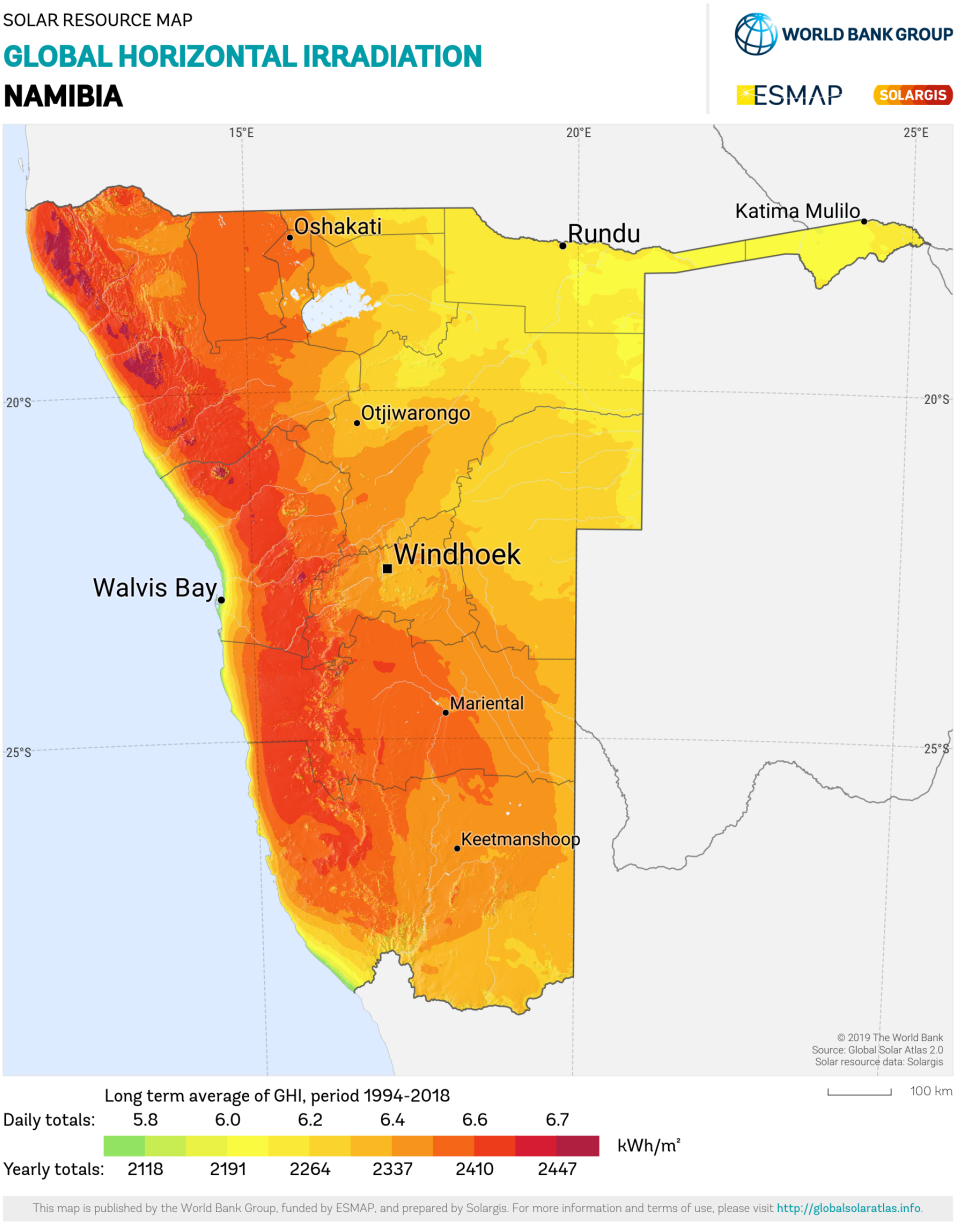

Figure 2.1: Global Horizontal Irradiation (GHI) Map of Namibia [1].

2.2 Bifacial vs Monofacial Solar Modules

Monofacial modules are traditional solar panels that have solar cells exclusively on their front side, while bifacial modules have solar cells on both the front and back sides [9]. The back cells generate additional power by capturing reflected light, resulting in higher overall energy output [10, 11]. Compared to monofacial PV modules, bifacial modules have shown energy yields of around 10% higher or more in the field depending on locations and environmental factors such as different albedos [12].

Lamers et al. (2018) investigated the temperature impacts on bifacial modules compared to monofacial modules and found that bifacial modules absorb significantly more heat from both sides due to light absorbed from both the front and rear sides. Despite this increased heat absorption, bifacial modules gain more energy than they lose from heating, and their effective heat transfer leads to better performance overall. Additionally, in certain environmental conditions such as moderate albedo conditions, the bifacial energy gain does not result in higher temperatures for the bifacial module compared to the monofacial module [13].

McIntosh et al. (2019) investigated mismatch loss in bifacial modules due to nonuniform illumination in single-axis tracking systems. The study found that non-uniform illumination causes an annual energy yield reduction of 0.23% for central modules and 0.35% for edge modules in a one-high bifacial tracking system [14]. The higher loss in edge modules occurs because they receive more intense but uneven rear-side illumination due to increased ground-reflected light and less shading from neighbouring modules. In contrast, central modules experience more uniform rear illumination, reducing current mismatch and resulting in lower losses. Factors like torque tube shading and ground albedo further amplify this difference [14].

Additionally, Rossa et al. (2021) found that mismatch losses in monofacial modules were 0.09%, increasing by 0.04% per year due to aging, while bifacial modules showed mismatch losses of 0.01% with rear side mismatch losses of 0.2%-0.4% due to the nonuniform rear irradiance [15].

Raina et al. (2021) carried out simulations to compare the performance of monofacial PV cells to bifacial Passivated Emitter and Rear Cell (PERC) PV cells, considering the effect of albedo on bifacial performance under STC conditions. The results of the study demonstrated that bifacial devices could achieve a higher energy yield with higher albedo values, potentially leading to a reduction in the levelized cost of electric-

ity (LCOE) [16]. While some studies indicate potential advantages of using bifacial modules in certain conditions, others highlight the importance of considering factors like mismatch loss and spatial variability in light distribution for the solar cells at the back.

While bifacial solar modules show promise in increasing energy output over traditional monofacial modules, further research is essential to determine the specific conditions under which they consistently outperform monofacial modules.

2.2.1 Structural Differences Between Bifacial and Monofacial Solar Modules

The standard monofacial module has 3 basic layers: glass, solar cells, and Tedlar Polyester Tedlar (TPT) back sheet. The solar cells in a monofacial module are set in an encapsulant which prevents moisture ingress into the module and a Tedlar back-sheet. The panel is able to absorb only sunlight falling on its top surface as the back sheet is not transparent. In a bifacial module, the Tedlar back sheet is replaced with a rear glass sheet. The cells of a bifacial module have busbars on both sides [17]. The differences in structures between the standard monofacial and bifacial solar cells are shown in Figure 2.2.

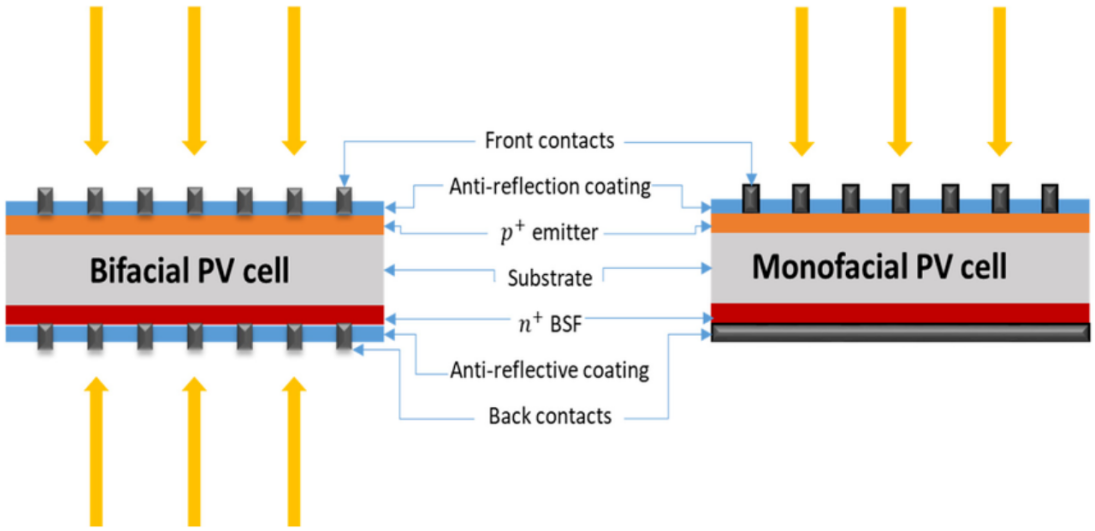

Figure 2.2: Monofacial and Bifacial Solar Cell

Bifacial modules are assumed to have an 8% relative efficiency advantage over monofacial modules, as stated in the Photovoltaic (PV) Module Technologies report [18]. Bifacial solar cells have been shown to have higher power performance compared to monofacial cells, with one significant reason being the mismatch between interconnected solar cells due to shading [19]. Bifacial photovoltaic (PV) modules show improved efficiency, as the photogenerated carrier profile in the absorber layer differs between bifacial and monofacial cells [20]. In monofacial solar cells, electrons and holes are primarily generated near the front surface where the light enters the semiconductor material. In contrast, in bifacial solar cells, they are generated more uniformly throughout the absorber layer because light enters from both sides. Deeper into the absorption layer of the monofacial solar cell, the carrier concentration decreases while the carrier concentration is more evenly distributed across the thickness of the absorber layer in bifacial solar cells.

Overall, the differences between bifacial and monofacial module technologies lie in their structural design and operational efficiency, with bifacial modules offering advantages in terms of efficiency and power performance.

2.2.2 Electrical Characteristics of Solar Modules

A monofacial solar module can be represented electrically by an equivalent circuit comprising a current source, one or two diodes, two resistors (series (R_s) and shunt (R_{sh})), and a load. As illustrated in Figures 2.3 and 2.4, the physical components of the equivalent circuits are identical. The key difference in the equivalent circuits of monofacial and bifacial solar cells is that the bifacial cell must account for the additional photocurrent generated from the rear side ($I_{ph,f}$ and $I_{ph,r}$).

The differences in monofacial and bifacial solar cell electrical circuits indicate different behaviours, particularly under shading and mismatch conditions. When shading occurs on a monofacial module, the affected cells produce less current, decreasing the overall power output of the module. In contrast, the rear side of bifacial solar cells can still capture reflected and diffused light when the front has been shaded, helping mitigate the shading effects by maintaining a higher overall current.

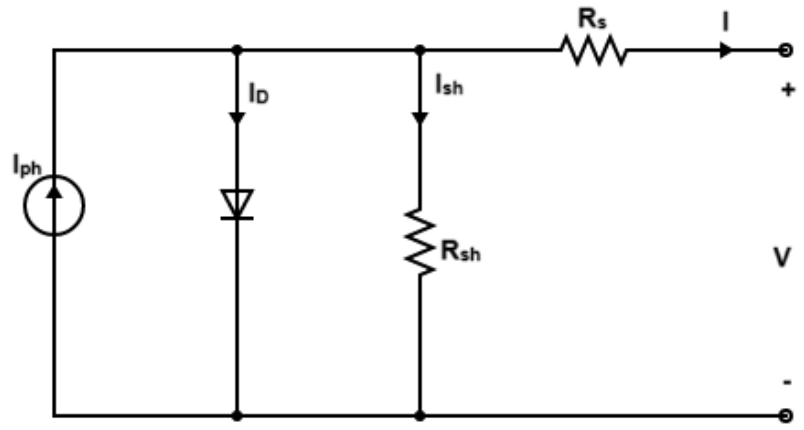

Figure 2.3: Monofacial Equivalent Circuit

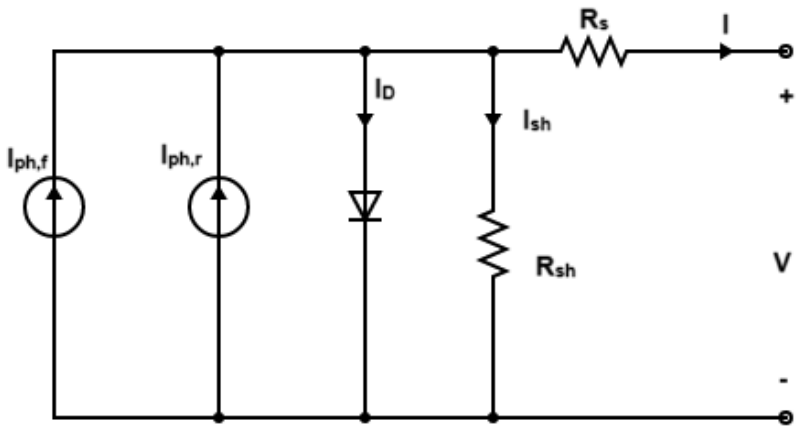

Figure 2.4: Bifacial Equivalent Circuit

1. Current-Voltage *(I-V)* Curve: The *I-V* curve, Figure 2.5 represents the relationship between the current (I) and voltage (V) of the module under different operating conditions. Various *I-V* curves exist; a translated *I-V* curve for photovoltaic (PV) systems refers to the adjustment of the measured current-voltage (IV) characteristics of a PV module or array to standard test conditions (STC), as shown

in Table. 2.1, which include normal incidence (solar radiation perpendicular to the surface of the solar cell), a solar cell temperature of 25°C, and the AM1.5 solar radiation spectrum (representing the solar spectrum after passing through the Earth's atmosphere at a 48.2° angle). This process is essential because the performance of PV modules varies with changes in irradiance and temperature.

By analyzing the *I-V* curve, important parameters such as the short-circuit current (I_{SC}), open-circuit voltage (V_{OC}), and fill factor (FF) can be determined. The I_{SC} represents the maximum current provided by the PV array. The open-circuit voltage is the maximum voltage output of the solar cell when no current is flowing. The fill factor (FF) is the ratio of the maximum power produced by a cell and the power it could have produced if it had no losses, and is an indicator of the quality of the cell. *I-V* curve measurements are essential for evaluating the performance of solar modules and can help identify any issues with the modules. By tracing the *I-V* curve, it is possible to determine the maximum power point (MPP) where the module operates most efficiently at the given conditions [21]. The current for the monofacial equivalent circuit is given by the following equation:

$$I = I_{ph} - I_D - I_{sh} = I_{ph} - I_D \left(e^{\frac{V+IR_s}{nV_t}} - 1 \right) - \frac{V + IR_s}{R_{sh}} \tag{2.1}$$

and the bifacial equivalent circuit:

$$I = I_{ph,f} + I_{ph,r} - I_D - I_{sh} = I_{ph,f} + I_{ph,r} - I_D \left(e^{\frac{V+IR_s}{nV_t}} - 1 \right) - \frac{V + IR_s}{R_{sh}} \tag{2.2}$$

Where:

I_{ph} = Photocurrent

$I_{ph,f}$ = Front photocurrent

$I_{ph,r}$ = Rear photocurrent

I_D = Voltage dependent current lost to recombination

I_{sh} = Current lost due to shunt resistance

V = Output Voltage

V_t = Thermal voltage

R_s = Series resistance

R_{sh} = Shunt resistance

n = diode ideality factor

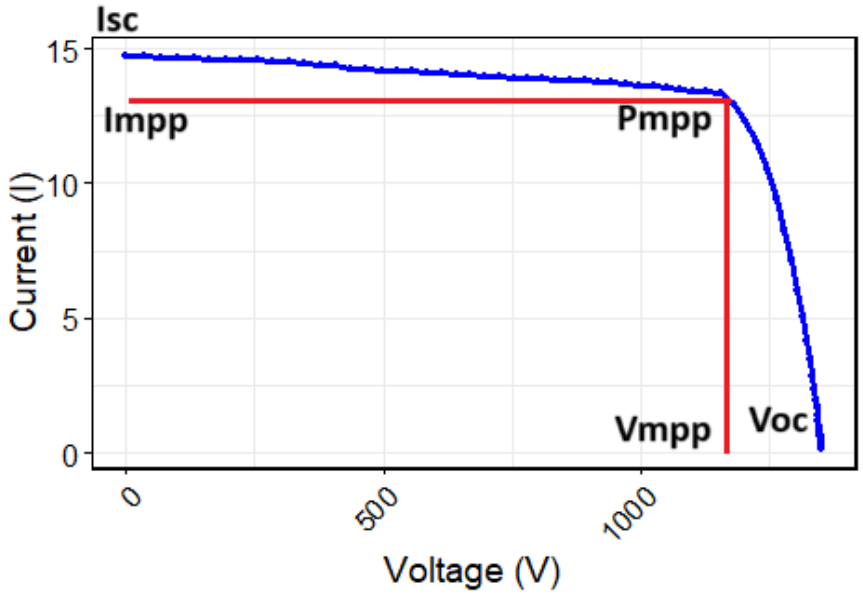

Figure 2.5: *I-V* Curve of a Solar Cell

2. Efficiency: The efficiency of a module is a crucial performance metric that indicates its ability to convert sunlight into electricity. Efficiency is calculated by dividing the module's power output by the incident solar power [22]. Efficiency measurements of monofacial modules and the front side of bifacial modules are performed under standard test conditions (STC) seen in Table 2.1.

Table 2.1: Standard Test Conditions (STC) for characterising PV modules

Variable	**STC Value**
Irradiance	1000 W/m^2
Temperature	25 °C
Air Mass	1.5

3. Light Intensity Effects: Current increases with light intensity. As more photons are absorbed, more electrons are freed, thus generating a higher current.

The I-V curve of a bifacial module's rear side is typically distorted because of several factors. Partial shading from the junction box, cabling, or the frame of the module can cause irregularities. Additionally, non-uniform illumination from the ground and surrounding reflections leads to variations in current generated in different cells and cell sorting since bifacial modules are typically sorted based on the front-side current only, this can result in mismatches that further distort the I-V curve.

The rear-side illumination of bifacial solar cells plays a crucial role in increasing the overall power output of the solar module. Research has shown that bifacial modules offer greater power output compared to conventional monofacial modules by harvesting light that is reflected off surfaces [11]. The rear side irradiance, which consists of light reflected from the ground and surrounding surfaces, significantly contributes to the overall power output, leading to higher energy production [23]. This is particularly effective in environments with high albedo, which refers to the proportion of solar radiation that is reflected by a surface, such as snowy or sandy areas, where the ground reflects more sunlight.

Studies [24–26] combining numerical device simulation with experimental data found that the power output of bifacial solar cells can differ by up to 30% from the power of monofacial cells when rear illumination is applied. This significant difference underscores the importance of rear-side irradiance in enhancing

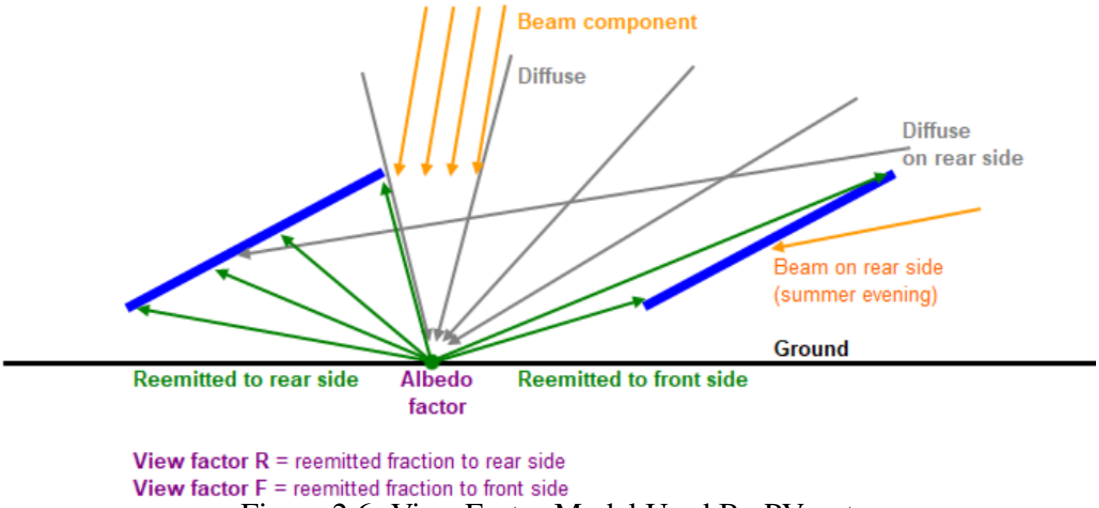

Figure 2.6: View Factor Model Used By PVsyst

the overall efficiency of bifacial modules. The study by Duran et al. (2011) also emphasises that the performance of bifacial modules is highly dependent on the installation environment and the amount of light available for the rear-side capture [26].

The non-uniformity of rear-side irradiance has been identified as a significant factor affecting power generation in bifacial PV systems [27]. By optimizing the rear-side layout and design of bifacial solar cells, researchers aim to achieve up to a 25% increase in annual yield [28].

Factors such as the view factor illustrated in Figure 2.6, which is the fraction of radiation leaving one surface that directly strikes another surface, play a crucial role in determining the overall power generation and efficiency of bifacial modules. The view factor helps determine the rear-side irradiance by considering the geometry of the installation, the albedo, and the positioning of the modules.

4. Bifaciality Factor: The bifaciality factor is a metric that describes the ratio of rear-side power output to the front-side power output used to assess the performance of bifacial solar cells [29]. It indicates how effectively the module utilises the rear-side for power generation. A higher bifaciality factor indicates a more efficient utilisation of the rear-side and a higher potential for bifacial gain. The bifaciality factor depends on factors, such as the type and quality of the silicon, the design and layout of the cells and modules, the transparency and spacing of

the modules, and the albedo of the ground or other surfaces behind the modules. Optimised designs can enhance light capture and reduce losses. Proper spacing and transparent materials can increase the amount of light reaching the rear side. Higher albedo surfaces reflect more light onto the rear side of the modules, boosting their performance. It is challenging to determine the bifaciality factor because it can be measured using either standard test conditions (STC) or under real-world conditions with different irradiance values. Under STC, the front side of the module is typically exposed to an irradiance of 1000 W/m2, while the rear side is exposed to a much lower, specified irradiance. These conditions provide a consistent basis for comparing the performance of different bifacial modules. However, real-world conditions often differ significantly from these test conditions, with factors such as angle of incidence, diffuse light, and albedo affecting the rear side irradiance. The bifacial factor is given by the following formula:

$$\text{Bifacial Factor} = \frac{\text{Rear-Side Efficiency}}{\text{Front-Side Efficiency}} \tag{2.3}$$

5. Temperature Coefficients: Temperature coefficients are the metrics which quantify how much a module's power output decreases with each degree Celsius increase in temperature above 25°C. Similar to monofacial modules, bifacial modules have temperature coefficients that describe the change in their electrical parameters with temperature [30]. Typically, bifacial modules have lower temperature coefficients than monofacial modules, meaning they are less affected by temperature increases. This is advantageous because it allows bifacial modules to maintain higher efficiencies in hotter climates. However, when bifacial modules receive radiation on both sides, their operating temperature can occasionally exceed that of monofacial modules. This potentially offsets some of the benefits of the lower temperature coefficient. Environments with good airflow can have a cooling effect which can help mitigate the higher operating temperatures and reduced performances, however, in stagnant air conditions, the higher irradiance can lead to increased temperatures and reduced performance. [31].

2.3 PV Systems

Grid-connected PV systems comprise 99.6% of the current global PV installed capacity [32]. The main components of these systems consist of solar panels, inverters, mounting structures, transformers, electrical components such as cables and fuses, and battery energy storage systems. Together, these components, excluding the solar panels, are known as the balance of system (BOS) of the plant.

Overall, the performance and efficiency of PV systems are intricately linked to system design choices and location-specific environmental factors such as albedo, and solar resource.

2.3.1 Fixed-Tilt PV Systems

A fixed-tilt PV system is a type of solar power system that uses solar panels that are mounted at a fixed angle and do not track the sun's movement. The fixed tilt angle is usually chosen to optimize the solar radiation that the panels can collect throughout the year.

A study by Chudinzow et al. (2020) explored the impact of design parameters such as row spacing, module elevation, tilt angle, and soil reflectivity on the performance of bifacial photovoltaic systems. It highlighted that optimising these parameters, particularly with larger row spacing and soil brightening measures, can significantly enhance energy yield and reduce the levelized cost of electricity (LCOE). It was found that fixed-tilt technology utilising bifacial modules can increase the energy yield by 5%-10% when paired with high-albedo surfaces [33]. This supports the claim that fixed-tilt technology is beneficial for bifacial systems.

2.3.2 Single Axis-Tracking PV Systems

An additional way to increase the amount of irradiation a solar module receives, thereby increasing the energy output of the system, is by sun-tracking using single-axis tracking.

Pelaez et al. (2018) found that bifacial modules in single-axis tracking systems can boost energy yield by 4%–15%, with a global average of 9% [34]. Similarly, Janssen et al. (2018) demonstrated through their mathematical model that monofacial and bifacial PV arrays with single-axis tracking can increase energy yield by 15% and 26%, respectively, compared to monofacial fixed-tilt systems [35]. Furthermore, Khan et al. (2021) discussed predictive modelling of energy yield, economics, and reliability for next-generation bifacial solar farms, predicting a 20%–30% energy gain for fixed-tilt bifacial modules and an additional 20%–40% gain for single-axis bifacial tracking within ±30 degree latitudes. A techno-economic assessment by Urs et al. (2023) of various configurations of photovoltaic systems for energy and hydrogen production identified single-axis tracking structures with bifacial PV modules as the most suitable configuration based on technical and economic performance for locations with different surface albedo values [36].

2.4 PV Modelling Techniques

There are three classes of models commonly used for modeling of PV systems: analytical, empirical, and simulation-based models. Analytical modeling methods that expresses a description of physical behavior of PV systems through mathematical equations or empirical modeling which is based on experimental data. Simulation-based models are developed through the use of software tools that combine empirical and analytical methods to provide a more holistic performance prediction. The software commonly used in both PV research and industry, include PVsyst, SAM (System Advisor Model), HelioScope, PVSol, AutoCAD, etc. PVsyst is recognised for its accuracy, acceptance in the industry, ease of use, and extensive meteorological database. It provides detailed loss analysis, simulation of different climatic conditions, a wider range of module brands, and includes a comprehensive financial analysis. PVsyst also stands out for its ability to generate complex shading scenarios, whereas SAM is often considered less user-friendly. HelioScope, though excellent for design purposes, lacks the detailed performance analysis features of PVsyst. PVSol provides robust simula-

tion capabilities but is not as widely accepted in the industry as PVsyst. AutoCAD is primarily used for design and layout purposes rather than performance modeling. PVsyst was selected for this study due to its high accuracy, widespread industry acceptance, and user-friendly interface, making it ideal for modeling PV systems in diverse climatic conditions and providing detailed insights into system losses and performance.

2.5 PV System Performance Metrics

The key performance metrics used to analyse the performance of a PV system are:

1. Specific Energy Yield: Energy yield measurements are necessary to predict and optimise the expected energy generation of PV plants. The energy yield is the actual total number of kilowatt-hours produced by an installed PV system in a year while the specific yield refers to how much energy (kWh) is produced for every kWp of module capacity over an actual year [10]. The specific energy yield is calculated using the following formula:

$$\text{Specific Energy Yield} = \frac{\text{Energy Produced (kWh)}}{\text{Installed Capacity (kWp)}} \tag{2.4}$$

2. Performance Ratio: The performance ratio represents the actual energy generated by the PV plant to its expected energy with reference to its nameplate rating, taking into consideration the losses [37]. Daher et al. (2018) evaluated the impact of ambient temperature on the performance of a PV power plant in Djibouti, noting a reduction in the performance ratio with increasing ambient temperature. Additionally, the performance ratio of a PV system is also affected by periods of system unavailability when system losses occur. System unavailability is the period of time during which the PV system is not operational or incapable of producing electricity due to maintenance activities, grid outages, or equipment failure [38]. The performance ratio is calculated using the following formula:

$$PR = \frac{E_{\text{Grid}}}{\text{GlobInc} \times P_{\text{nomPV}}} \tag{2.5}$$

Where:

$$E_{Grid} = \text{Available Energy}$$

$$GlobInc = \text{Incident global irradiation in the collector plane}$$

$$P_{nomPV} = \text{STC installed power (manufacturer's nameplate value)}$$

3. Financial Aspects: PV solar systems offer low operation and maintenance costs compared to other renewable energy technologies, making them an attractive investment option [39]. By analyzing financial aspects such as the levelized cost of electricity (LCOE), payback period, and return on investment (ROI), stakeholders can make informed decisions about the financial viability of PV projects and assess whether or not it would be a profitable investment.

   The LCOE is the cost per unit of delivered electricity. The LCOE can be calculated as follows:

$$LCOE = \frac{\sum_{t=0}^{n} \frac{C_{0_t} + C_{OM_t}}{(1+i)^t}}{\sum_{t=0}^{n} \frac{E_t}{(1+i)^t}} \tag{2.6}$$

Where:

$$C_{0_t} = \text{Capital expenditure in year } (t)$$

$$C_{OM_t} = \text{Operations and maintenance cost in year } (t)$$

$$E_t = \text{Energy generated in year } (t)$$

$$i = \text{Discount rate}$$

$$t = \text{Year of the project}$$

The payback period is the number of years it would take for a project to break even or it can be defined as the year when the cumulative present value of net cash flow (NPV) becomes positive. The payback time can be calculated as follows:

$$\text{Payback Period} = t_b + \left(\frac{A_u}{A_{tr}}\right) \tag{2.7}$$

Where:

$t_b =$ time before break even (in years)

$A_u =$ Unrecovered amount in the year before NPV becomes positive

$A_{tr} =$ Cash flow in the recovery year

The ROI of a project is the discount rate at which the net present value (NPV) of the project is equal to 0. It measures the return generated on an investment relative to its cost and indicates the cost of the capital that can be sustained by the project. The higher the ROI, the more favourable the investment is.

2.6 Loss Factors

To get a more accurate estimate of the systems' energy and financial performances, losses must be taken into account when estimating how much energy a PV system will produce and which PV system will be most beneficial between a monofacial and bifacial PV system. The different loss factors can be categorised into environmental influences, PV system influences, PV installation factors, PV system cost issues and miscellaneous factors category [40].

Loss factors such as soiling, high temperatures, and harsh weather conditions can significantly impact the performance of solar modules. Soiling, caused by dust and dirt deposition, has been identified as a major issue affecting photovoltaic (PV) power generation in desert environments [41]. Studies have shown that soiling can lead to substantial loss in solar panels, reducing the amount of irradiance reaching the solar cells and ultimately reducing the power output delivered by the modules [42].

Research carried out by Stanka et al. (2020) [43] indicated that PV module performance can be adversely affected by temperature increases. The study found that power losses were up to 12.63 W/m^2 when the temperature of the PV modules reached 53.5°C [43]. This highlights the importance of considering environmental factors such as temperature and weather conditions when assessing the performance of solar modules.

The solar resource decreases with increasing latitude [44]. The choice of components in system design significantly impacts the energy yield of a PV system [45]. The electrical design of a solar system, including module stringing, conductor sizes, and cable cross-sections can impact wire losses and inverter efficiency [45]. Additionally, another important factor that affects solar module performance is albedo.

Ground reflectivity, known as ground albedo, is a critical factor affecting the performance of bifacial solar PV systems. Optimising the tilt and azimuth angles based on the panel location is essential for achieving the best energy output from solar panels. The spectral and angular distribution of solar radiation can impact albedo, influencing the amount of sunlight absorbed by solar panels. Furthermore, spectral albedo can have a positive effect on the potential power conversion efficiency of bifacial solar cells [29]. If all the incident light is reflected, the albedo equals to 1 [46]. More light will be reflected from a surface having a high albedo than one with a low albedo. Sand, snow, and ice, as well as some urban surfaces like concrete, have high albedos [46]. Forests, water, and some urban surfaces like asphalt are examples of surfaces having low albedos as seen in Table 2.2.

Table 2.2: Albedo values on different surfaces

Surface Type	Typical Value
Fresh asphalt	0.03-0.04
Open ocean	0.06
Worn asphalt	0.12
Sand	0.15-0.45
Agricultural crops	0.18-0.25
Bare soil	0.17
Green grass	0.20-0.25
Desert sand	0.30-0.40
Snow	0.40-0.90
fresh snow	0.80-0.90

2.7 Degradation

The energy output of modules decreases with age as the modules degrade over time. Degradation rates are provided by manufacturers in the module datasheets and are given in percentage per year. However, research has shown that in field conditions, modules degrade at faster rates than indicated by their datasheets. The degradation rate found is between 0.6% and 0.7% for the monofacial solar modules and 1.2% for the bifacial solar modules [47–49]. In correspondence with the module warranties, PV systems' lifetimes are typically set to 25 years and linear degradation with time is assumed.

Chapter 3

Methodology

This chapter details the workflow for modeling 3MW PV systems in PVsyst, including fixed-tilt and single-axis tracking configurations. Steps include incorporating site parameters, component selection, shading analysis, and loss factor customisation. The bifacial simulation methodology is elaborated using the Perez model and view factor calculations. Statistical and financial analysis methods (t-tests, LCOE, IRR) are also outlined.

3.1 System Modelling

The systems were modelled using PVsyst. The steps required to design the model in the software program were:

1. System type and location specification: The location of the site was specified using latitude and longitude coordinates. PVsyst utilises a built-in meteorological database, Meteonorm, that provides site-specific climatic data used to accurately simulate the performance of PV systems. The software offers default values for various parameters, however, for this study, parameters such as albedo were customised based on literature to better suit the site specifications [50]. Own measured meteorological data can also be imported into PVsyst for greater accuracy for models.

2. System Design: The plant orientation of the PV system can be configured as either fixed-tilt or axis-tracking. For this study, a fixed-tilt and single-axis tracking orientation was selected. The PV modules, inverters, and other components are then selected from PVsyst's extensive database. In PVsyst, the system losses include ohmic losses, soiling losses, thermal losses, resistive losses, light-induced degradation, and losses due to system unavailability. For this study, soiling rates, ohmic losses, and the system unavailability parameters were user-defined based on site-specific data and literature.

   To account for shading, a 3D scene was constructed. This involves creating a virtual model of the physical environment where the PV system will be installed. This gives a more accurate picture of any potential shading within the area.

   PVsyst also allows users to create multiple variants of a system within the same project. This allows users to optimise designs.

3. Once the design is complete, detailed hourly simulations are generated. After accounting for all losses and system performances, a comprehensive report is generated.

3.1.1 Bifacial Simulation

The irradiance reaching the front and rear surface of bifacial solar modules is calculated using the comprehensive Perez model and view factor. The accurate assessment of light incident on the front and rear surface of the module includes:
Solar irradiance comprises three primary components: direct irradiance, which refers to the amount of solar radiation that reaches the Earth's surface in a straight line without being scattered or absorbed by the atmosphere; diffuse irradiance, which is scattered light from the sky; and ground-reflected irradiance, originating from sunlight

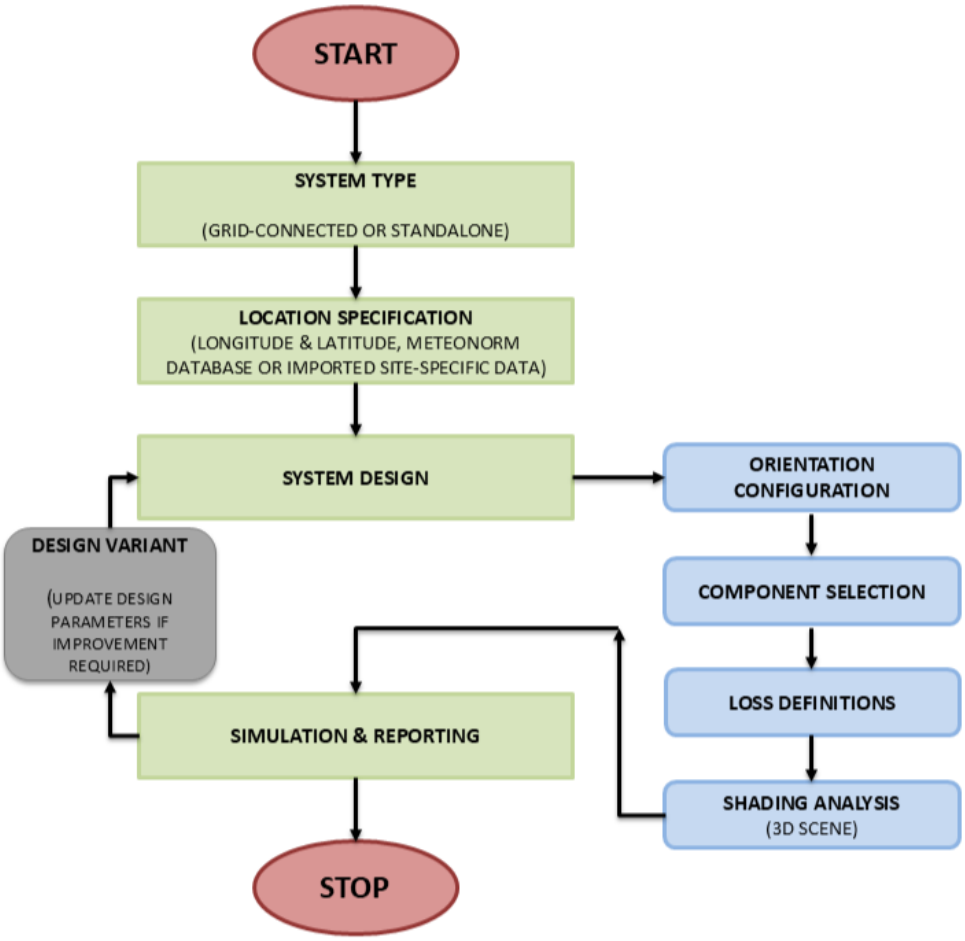

Figure 3.1: PVsyst Design Flowchart

bounced off the ground and modulated by albedo, a measure of surface reflectivity. These components collectively determine the total energy incident on photovoltaic modules, with ground-reflected irradiance playing a critical role in bifacial systems due to its dependence on albedo variations.

The model uses view factors to determine how much light is scattered back to the rear side of the module [51]. The view factor is the fraction of light re-emitted from a ground point that reaches the PV module. It assumes regular rows of modules with the same orientation and spacing, making it suitable for large-scale installations. The rear side irradiance is adjusted by the bifaciality factor, which accounts for the reduced efficiency on the rear side. Finally, the combined irradiance is used in the single-diode model to calculate the PV power output using Eq. (2.2).

Since actual real-time data is proprietary, the data (ohmic losses, soiling losses, unavailability, meteorological data) used in this study was simulated and taken from previous studies (albedo). The only measured data includes the I-V curves and the lengths between rows. Detailed module specifications can be found in Appendix A.1.1 and A.1.2. The global horizontal irradiance was found to be 2380 $\mathrm{kWh/m^2/year}$ at an optimal tilt angle of 22.3° at a latitude of 22.3175°S and longitude of 17.0425°E.

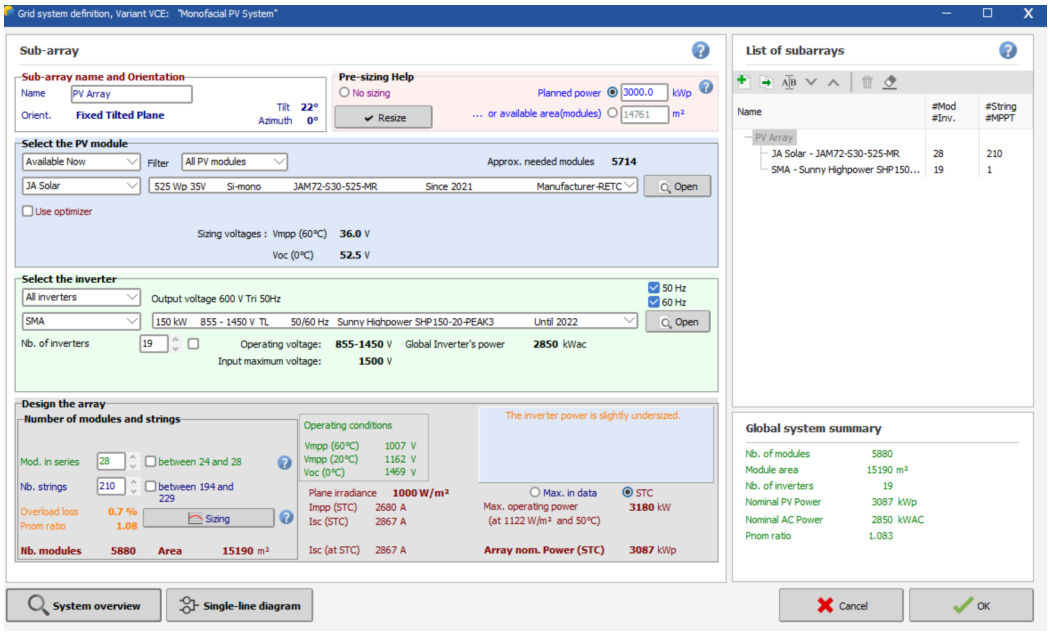

(a) Monofacial

(b) Bifacial

Figure 3.2: Screenshot from PVsyst showing Fixed-Tilt PV System Designs

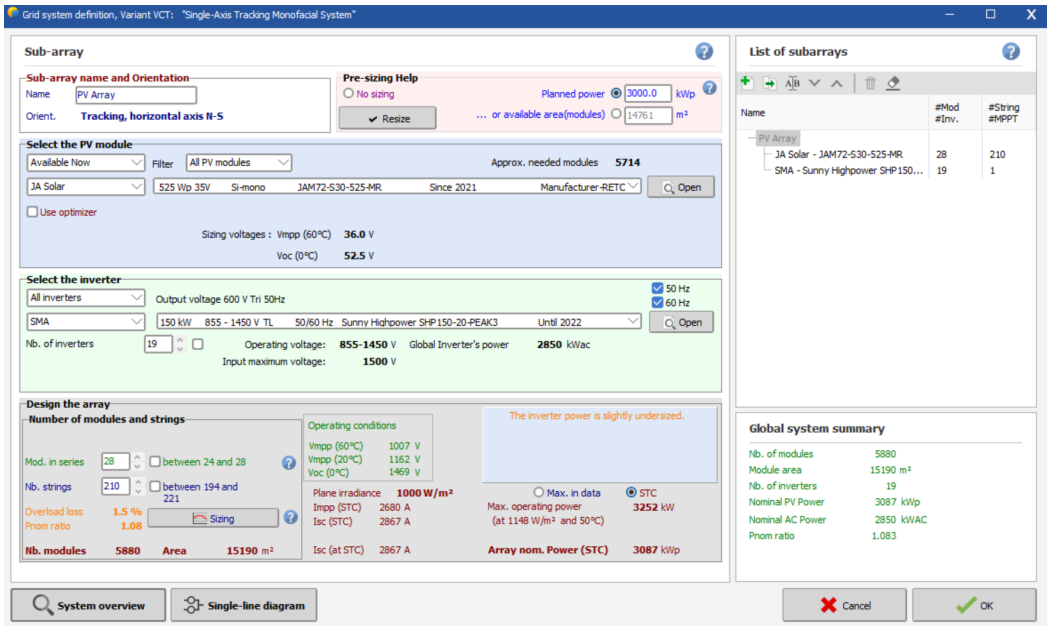

(a) Monofacial

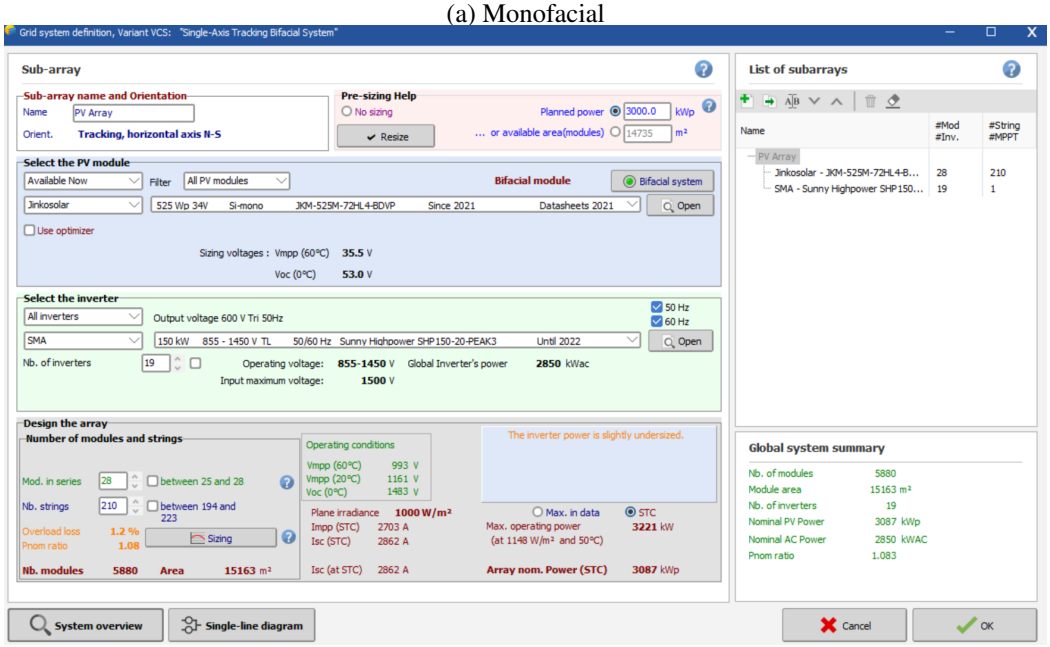

(b) Bifacial

Figure 3.3: Screenshot from PVsyst showing Single-Axis Tracking PV System Designs

There were 28 design variants simulated for each PV system design, with detailed cycles of improvements applied to achieve more accurate results.

The system design parameters can be seen in Fig. 3.2 and Fig. 3.3.

3.2 Data Analysis

1. Comparative assessment of the energy production of the systems was with RStudio using the t-test. This statistical test compares two group means to assess if their difference is statistically significant or if it could occur by random chance, using hypothesis testing. Independent samples t-test was used.

   The p-value of the t-test is the probability value that represents the likelihood of obtaining the observed data, assuming the null hypothesis is true. The significance value was taken to be 0.05 which is a commonly chosen threshold for significance.

2. The soiling losses were determined by comparing the measured *I-V* curves and the normalised *I-V* curves from two inverters at the site. For a more accurate model, it was assumed that the soiling loss would be halved during the rainy season (November-April). To calculate the soiling loss from measured *I-V* curves, the performance of a soiled solar panel is typically compared to a clean reference panel. The soiling loss can be expressed as a percentage loss in power output per day. The soiling loss was calculated using Eq. 3.1, [52]:

$$\text{Soiling loss} = \frac{Pmax_{\text{clean}} - Pmax_{\text{soiled}}}{Pmax_{\text{clean}}} \times 100 \tag{3.1}$$

   Where:

$$Pmax_{clean} = \text{maximum power output of the clean reference panel}$$

$$Pmax_{soiled} = \text{maximum power output of the soiled panel}$$

3. It is not possible to account for the tracker power consumption when there is no storage available in the software; this adjustment needs to be done manually after the simulation is completed.

4. The profitability of an investment in a PV system is evaluated using various financial metrics, including the levelized cost of electricity (LCOE), cash inflow, capital expenditure (CAPEX), operational expenditure (OPEX), net cash flows, present values, cumulative present value of net cash flow, discounted energy, discounted capital expenditure, discounted operational expenditure, internal rate of return (IRR), net present value (NPV), and payback periods. These metrics are calculated to assess the economic performance of a PV system, using the following equations:

Energy (kWh):

$$\text{Energy}_t = \sum_{t=0}^{n} (\text{Yearly energy production} \times (1 - \text{Degradation Rate})^t) \tag{3.2}$$

Eq. 3.2 accounts for the degradation rate of the module over time.

Cost of Electricity (N$/kWh):

$$\text{Cost of Electricity}_t = \sum_{t=0}^{n} (\text{electricity tariff cost} \times (1 + \text{Inflation Rate})^t) \tag{3.3}$$

Eq. 3.3 adjusts the electricity tariff for inflation over time.

Cash Inflow (N$):

$$\text{Cash Inflow}_t = \sum_{t=0}^{n} (\text{Energy}_t \times \text{Cost of Electricity}_t) \tag{3.4}$$

Eq. 3.4 calculates the cash inflow based on the cost of electricity and the energy production.

OPEX (N$):

$$\text{OPEX}_t = \sum_{t=0}^{n} (\text{Initial OPEX} \times (1 + \text{Inflation Rate})^t) \tag{3.5}$$

Eq. 3.11 adjusts the operational expenditure costs for inflation over time.

Net Cashflow (N$):

$$\text{Net Cashflow}_t = \sum_{t=0}^{n} (\text{Cash Inflow}_t - \text{CAPEX}_t - \text{OPEX}_t) \tag{3.6}$$

Eq. 3.6 calculates the net cashflow by subtracting the CAPEX and OPEX from the cash inflow.

Present Value of Net Cash Flow (N$):

$$\text{Present Value of Net Cash Flow}_t = \frac{\text{Net Cashflow}_t}{(1+i)^t} \tag{3.7}$$

Eq. 3.7 discounts the net cash flow to present value using the discount rate i.

NPV of Net Cash Flow (N$):

$$\text{NPV of Net Cash Flow}_t = \sum_{t=0}^{n} \frac{\text{Net Cashflow}_t}{(1+i)^t} \tag{3.8}$$

Eq. 3.8 sums the discounted present value net cash flows over time.

Discounted Energy (kWh):

$$\text{Discounted E}_t = \frac{\text{Energy}_t}{(1+i)^t} \tag{3.9}$$

Eq. 3.9 discounts the energy to the present value.

Discounted CAPEX (N$):

$$\text{Discounted CAPEX}_t = \frac{\text{CAPEX}_t}{(1+i)^t} \tag{3.10}$$

Eq. 3.10 discounts the capital expenditure to the present value.

Discounted OPEX (N$):

$$\text{Discounted OPEX}_t = \frac{\text{O\&M}_t}{(1+i)^t} \tag{3.11}$$

Eq. 3.11 discounts the operational expenditure to the present value.

The systems were modelled according to the Windhoek business' site specifications. The site can be seen in Fig. 3.4 located at system latitude of 22.3175°S and longitude of 17.0425°E.

(a) (b)

Figure 3.4: Bifacial tracking system at the site of the Windhoek business.

LCOE (N$/kWh) is calculated using Eq. 2.6. The inflation rate used in all the financial metrics is the historical financial rate calculated as an average over the past 10 years from 2013-2023. The discount rate is the fixed deposit rate from local national banks. The discounted CAPEX which has to take into account inverter replacement half-way through the project lifetime, discounted OPEX and discounted energy is used in the calculation of LCOE.

The IRR was calculated iteratively by varying the discount rate in steps of 0.25% to calculate different present values of the net cash flow. The discount rate at which the net present value is equal to 0 is known as the internal rate of return (IRR).

Chapter 4

Results and Discussions

Presenting simulation outcomes, this chapter compares energy yields, performance ratios, and financial metrics (LCOE, payback periods) across four system designs. Fig. 3.2a and 3.3b visualise the designs, while loss diagrams and NPV curves (Fig. 3.3a and 3.3b) quantify efficiency trade-offs. The discussion contextualises results against literature, addressing why bifacial systems underperform financially in Windhoek despite higher yields.

4.1 System Models

As shown in Fig. 4.1, the weather conditions on site can be seen as follows with the yearly global irradiation (GHI) is $2380\,\mathrm{kWh/m^2/year}$, imported via PVsyst using Meteonorm. The design characteristics in Table 4.1 generate the site temperature and monthly irradiation values in fig. 4.1. An increase in irradiation increases power generation; however, an increase in temperature increases resistance within solar cells, decreasing their output voltage and subsequently decreasing the power output of the cell [21].

The type of bifacial module used in the designs is the JinkoSolar JKM-525M-72HL4-BDVP module used in the actual systems by the business. The monofacial module type used is JA Solar JAM72-S30-525-MR, another well-regarded brand, due to its close resemblance to the bifacial module in terms of electrical parameters and specifi-

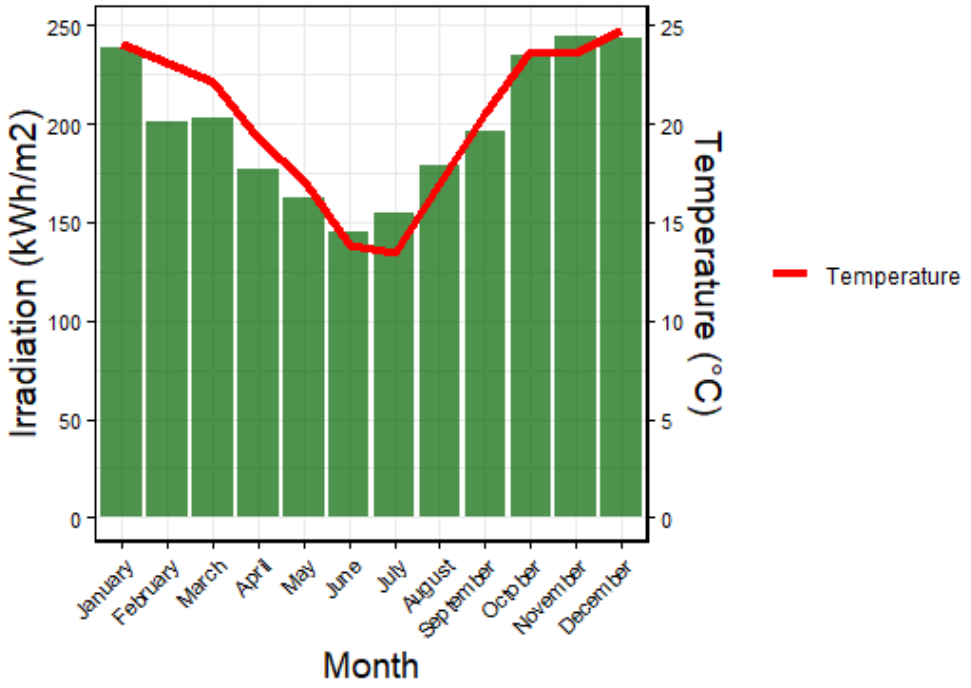

Figure 4.1: Average Site Temperature and Monthly Irradiation

cations. Both types of modules share nearly identical characteristics, with the monofacial module having a module efficiency of 20.3% compared to 20.36% for the bifacial module. Their rated maximum power is the same at 525 Wp, while the open-circuit voltage is 49.15V for the monofacial module and 49.42V for the bifacial module. Additionally, the short-circuit current is 13.65A for the monofacial module and 13.63A for the bifacial module. These similarities ensure a fair comparison between the two technologies. Additionally, both the monofacial and bifacial module types used in the designs are half-cell modules that provide better performance, reducing shading losses compared to full-cell modules. The modules both consist of P-type monocrystalline cells. The JA Solar module is used only to model the fixed-tilt and single-axis tracking systems with monofacial modules, while Jinkosolar is used to model the systems using bifacial modules. The datasheets for both modules can be found in Appendix Bifacial Module DataSheet and Appendix Monofacial Module Datasheet.

The inputs required for the system models are given in Table 4.1. System metrics such as albedo and soiling were user input. The datasheets for the system components are given in Appendix Datasheets.

Figure 4.2 illustrates the connections between the components of the systems modelled. It shows the string and inverter connections.

Table 4.1: Design characteristics of bifacial and monofacial PV systems

Parameter	Bifacial PV System	Monofacial PV System
Latitude	22.3175° S	22.3175° S
Longitude	17.0425° E	17.0425° E
Tilt	22.3°	22.3°
Azimuth	0°	0°
PV module model	525kW Jinkosolar JKM-525M-72HL4-BDVP	525kW JA Solar JAM72-S30-525-MR
Number of modules	5880	5880
PV module configuration	28 modules in series x 210 strings	28 modules in series x 210 strings
Inverter model	SMA Sunny Highpower SHP150-20-PEAK3	SMA Sunny Highpower SHP150-20-PEAK3
Number of inverters	19	19

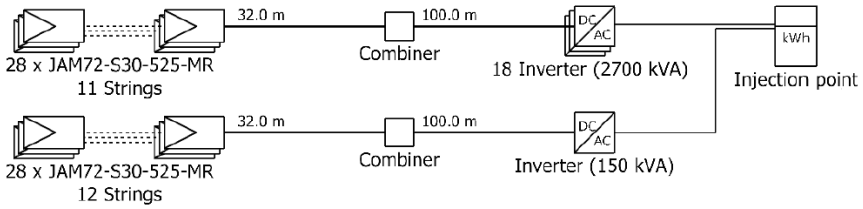

Figure 4.2: Simplified schematic (single-line diagram) showing the number of strings, and cable lengths to combiner boxes and to inverters

Figure 4.3 shows the modelled 3-D scene and its corresponding sunpath diagram with shading losses, where the panels are aligned along the north-south axis and track the sun from east to west. This system experiences no shading throughout the entire year. Figure 4.4 shows The modelled fixed-tilt 3-D scenes where the panels are placed on the east-west axis facing true north at a tilt angle of 22.3°, corresponding with the location's latitude. The fixed-tilt systems experience shading losses throughout the entire year due to inter-row shading.

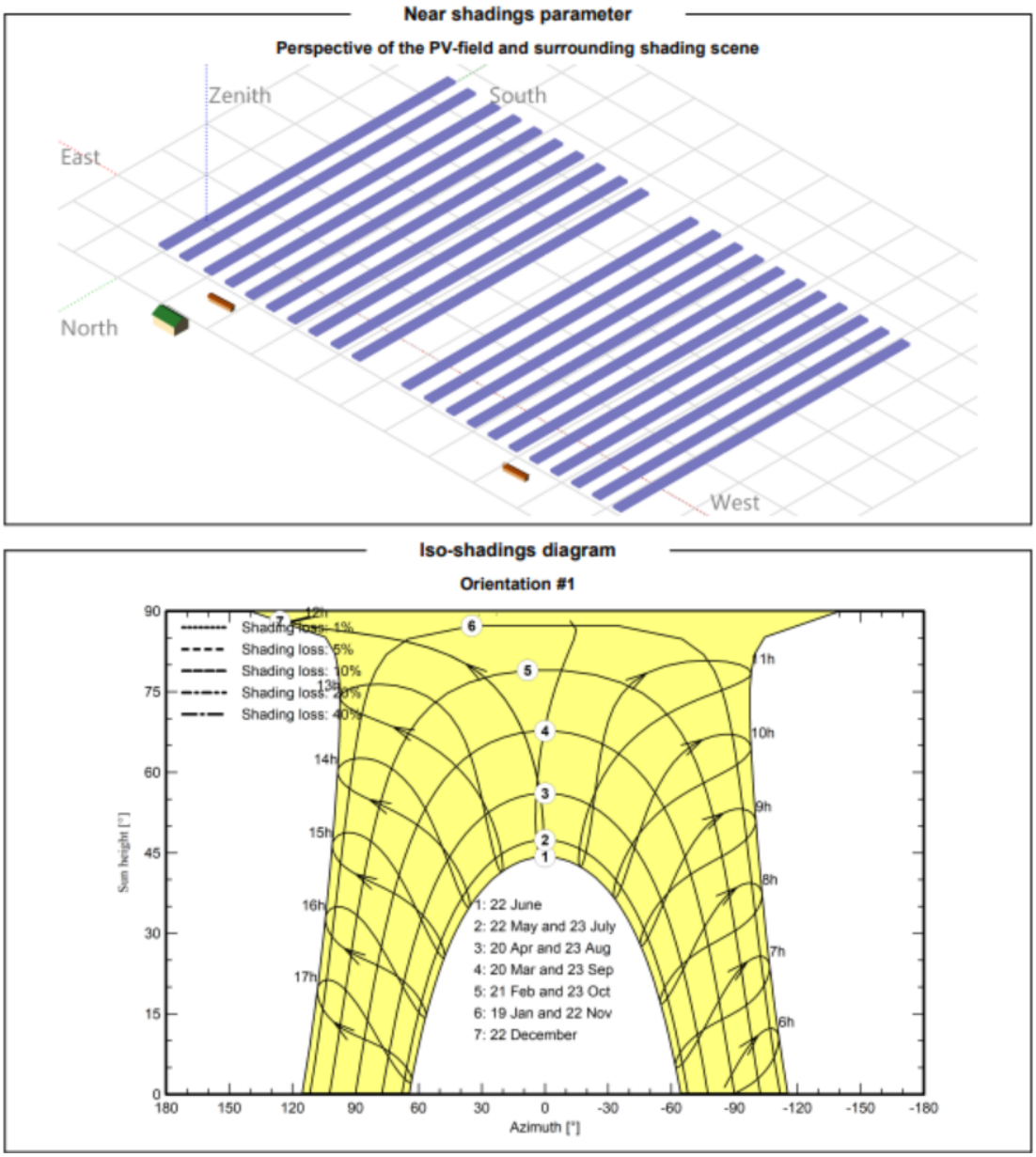

Figure 4.3: Single-Axis Tracking System 3D Scene and Sunpath Diagram with shading losses

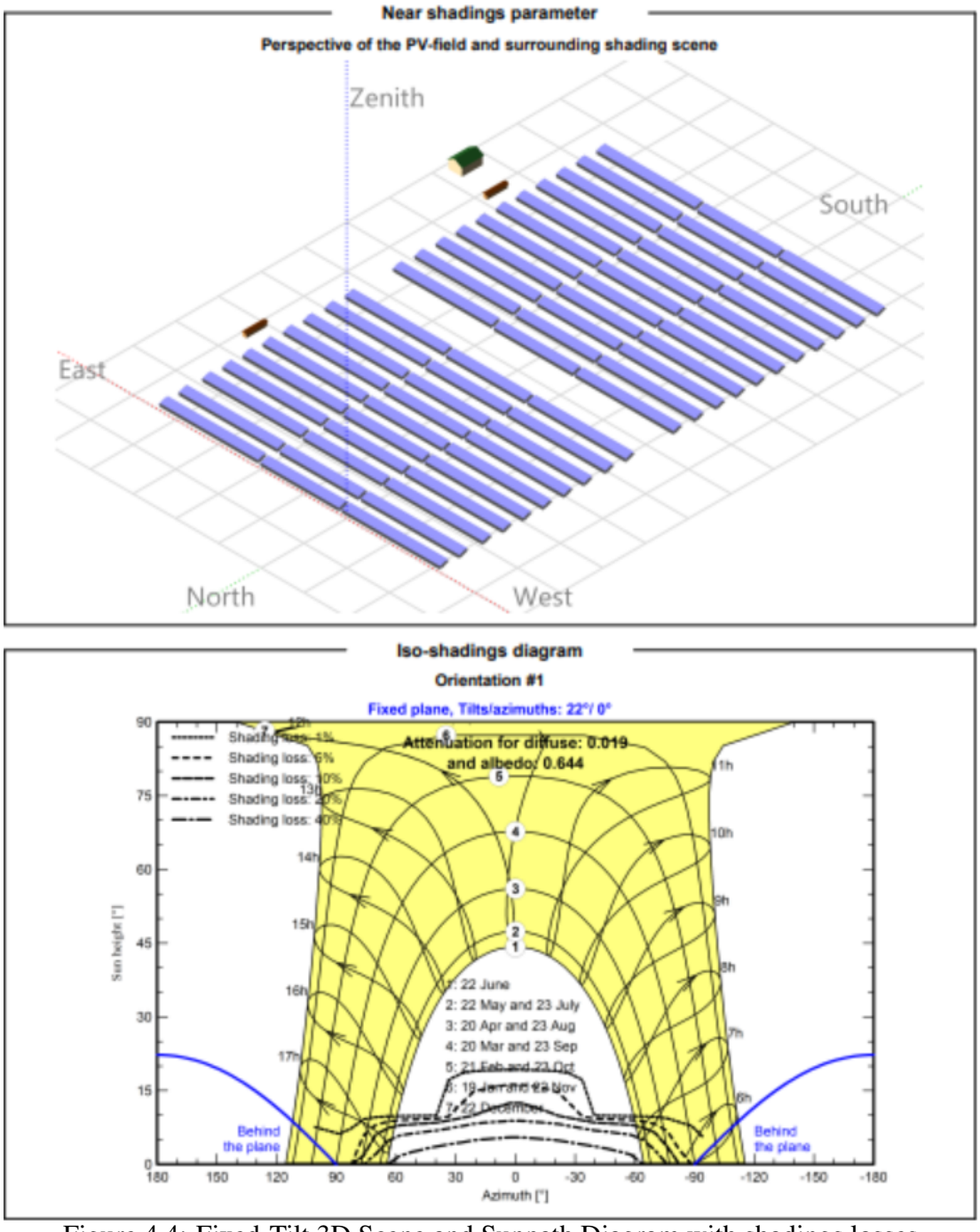

Figure 4.4: Fixed-Tilt 3D Scene and Sunpath Diagram with shadings losses

The modelled systems had soiling losses of 8.6% during dry seasons and 4.3% in rainy seasons, by comparisons of the I-V curves of two inverters on-site shown in Fig. 4.5 using Eq. (3.1).

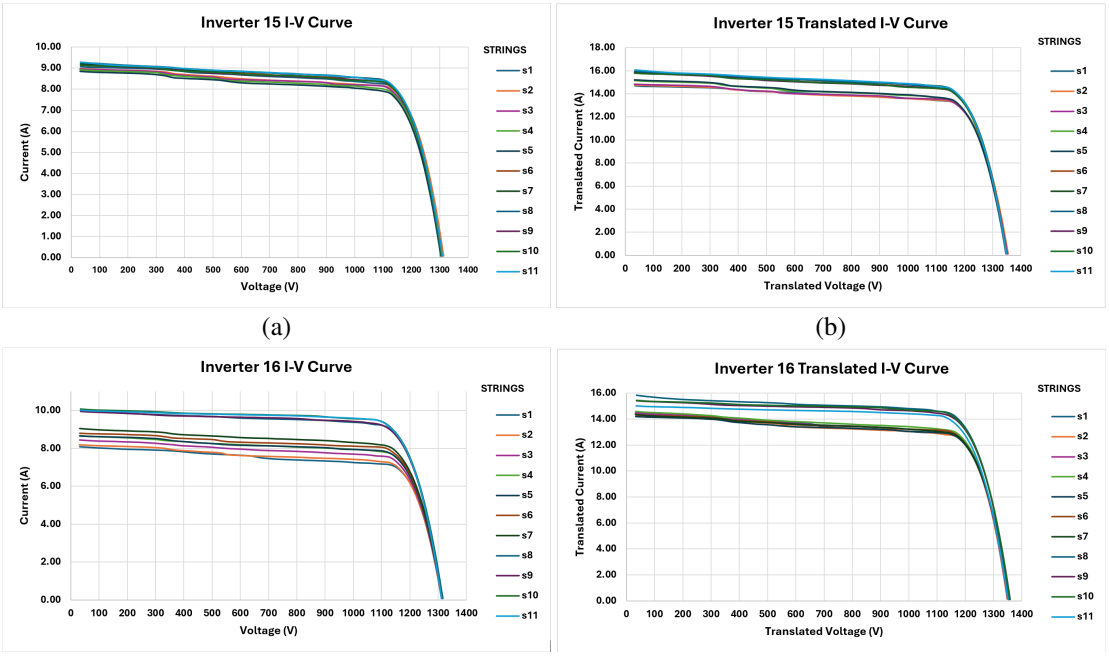

Figure 4.5: Measured *I-V* Curves. Image (a) shows the *I-V* curve of inverter 15. Image (b) shows the translated *I-V* curve of inverter 15. Image (c) shows the Inverter 16 *I-V* curve of inverter 15. Image (d) shows the translated *I-V* curve of inverter 16.

The monthly albedo values are based on a reference paper with monthly albedo values for Namibia from a study focusing on the performance of bifacial and monofacial PV modules in 55 different locations, with values graphed in Fig. 4.6 [50]. Accurate monthly readings of the albedo at the site could not be ascertained. The albedo decreases the most during the winter months, especially in July, due to clearer skies and lower irradiance levels. With reduced cloud cover, more sunlight reaches the ground, but the dry winter conditions expose darker, less reflective surfaces like bare soil that absorb more radiation. Additionally, the lower sun angle during winter increases atmospheric scattering of shorter wavelengths while allowing more absorption of longer wavelengths by surfaces, further reducing reflectivity. This seasonal albedo variation affects local energy balances and solar PV performance by altering the amount of reflected light available for bifacial systems, impacting the performance of PV systems. Higher albedo values result in more ground-reflected radiation, which increases the incident radiation on the rear side of bifacial modules, enhancing their energy yield.

Conversely, lower albedo values reduce the amount of reflected radiation, decreasing the overall energy production of bifacial modules. Understanding these variations is crucial for accurately modeling and optimizing PV system performance in different seasonal conditions.

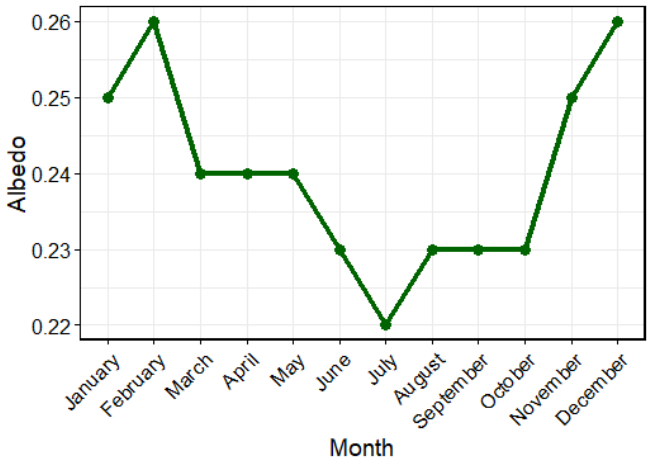

Figure 4.6: Monthly Albedo

The average cable length taken was 32 m/circuit (4 mm^2) from the string module connections and 100m/circuit (50 mm^2) from the main box to the inverter. The ohmic losses for the system was 2.695$m\Omega$. The system had 3 unavailability periods that lasted 36 hours each which totalled 4.5 days/year of unavailability. The height from the ground to the panel was taken as 2.27m and the distances between the rows ranged between 11.28m and 12.65m with a distance of 28m from rows 10 and 11. These values were measured on-site to replicate the site conditions. The self-consumption power of the trackers was calculated as 1822.58 kWh/month.

4.1.1 System Performance

The energy yield of the single-axis tracking PV systems is as shown in Fig. 4.7. However, as displayed in Fig. 4.15, the fixed-tilt PV systems do not follow the same trend. In the fixed-tilt systems, the dip in solar energy due to reduced irradiation is less significant than the dip in irradiation itself, primarily because of how the Plane of Array (POA) is calculated. POA irradiance accounts for direct, diffuse, and reflected compo-

nents, which can mitigate the effects of reduced irradiation on solar energy production. This means that even with lower irradiation in the winter months, the POA does decrease proportionally because of the tilt angle selected as shown in Fig. 4.8, allowing for optimised performance of the system throughout the year.

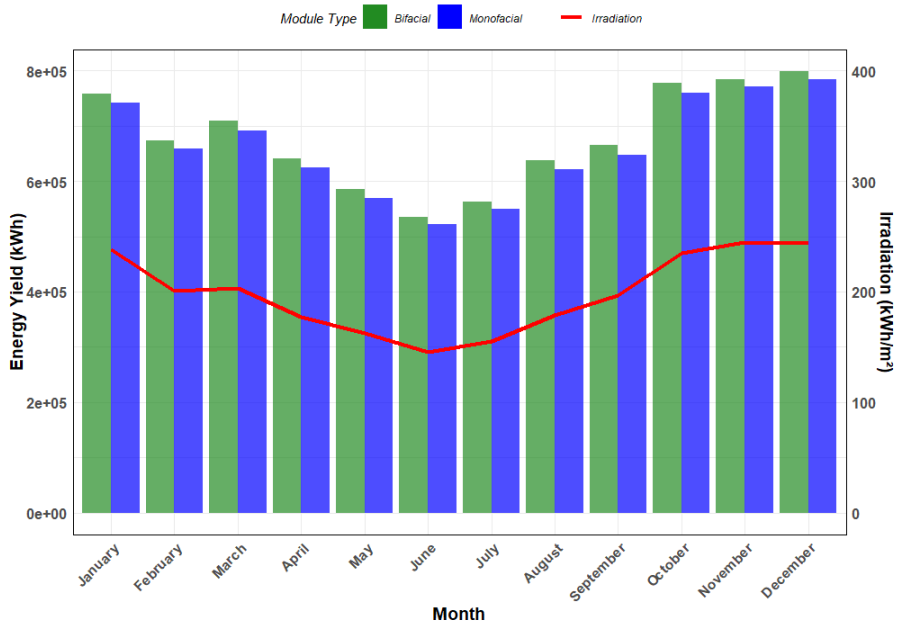

(a)

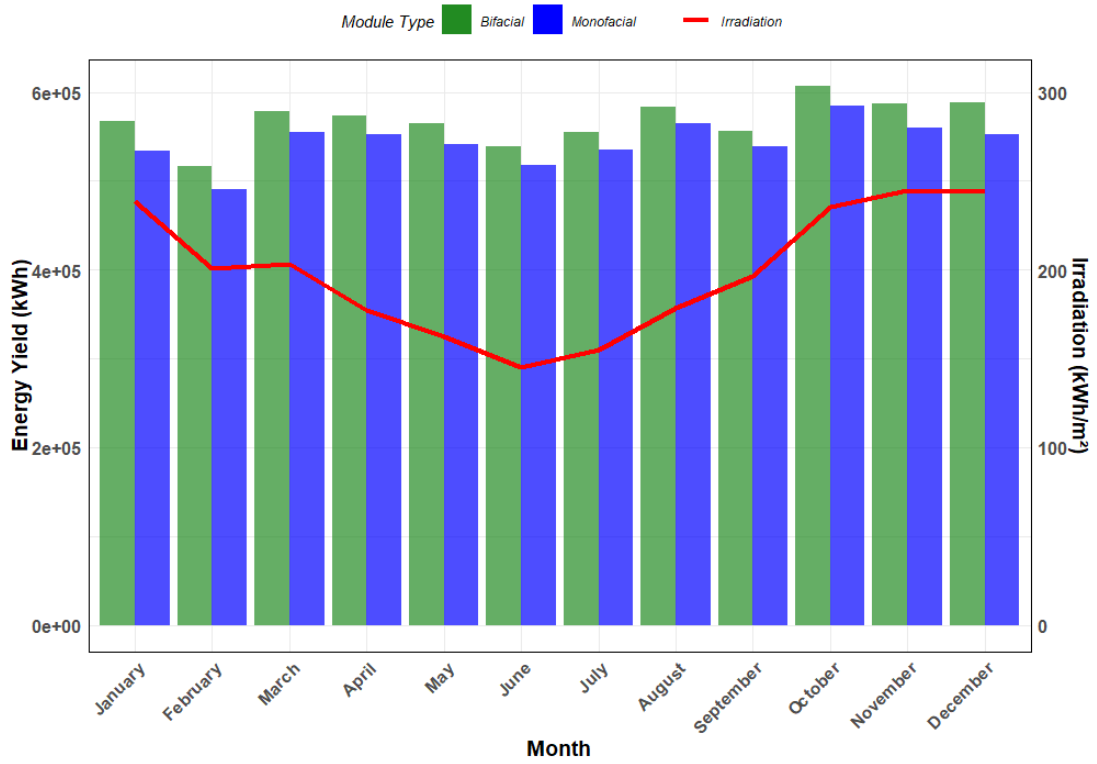

(b)

Figure 4.7: PV System Energy Yield & Irradiation. Image (a) shows the single-axis tracking monofacial and bifacial PV systems energy Yield & irradiation and (b) shows the fixed-tilt monofacial & bifacial PV systems energy Yield & irradiation

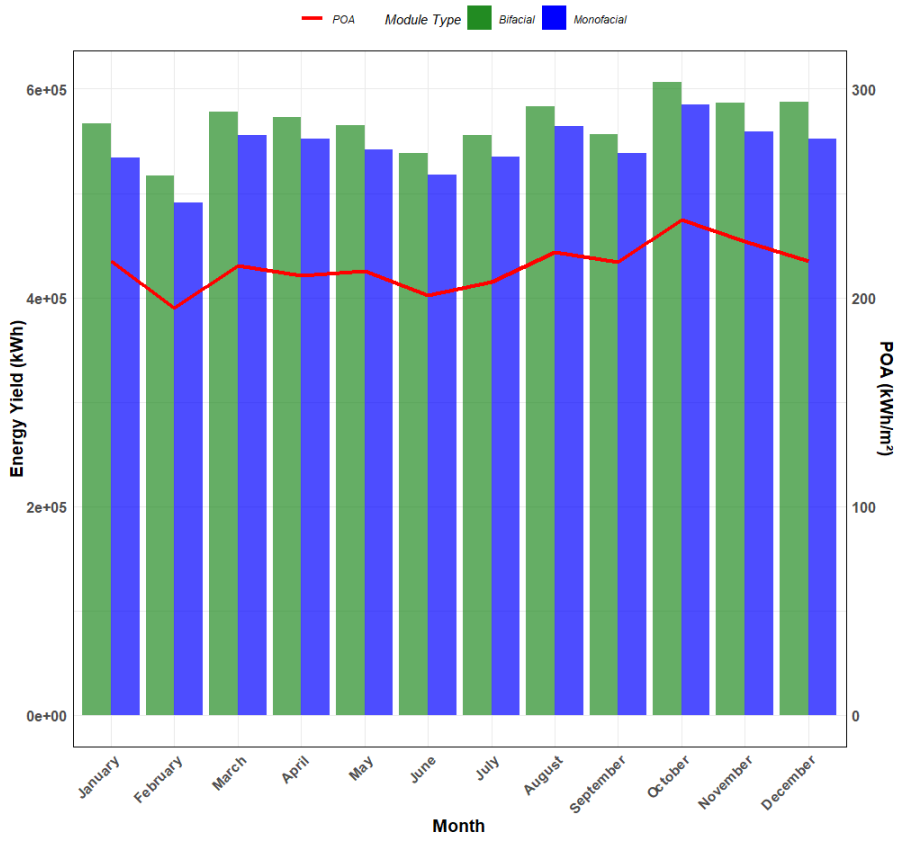

(a)

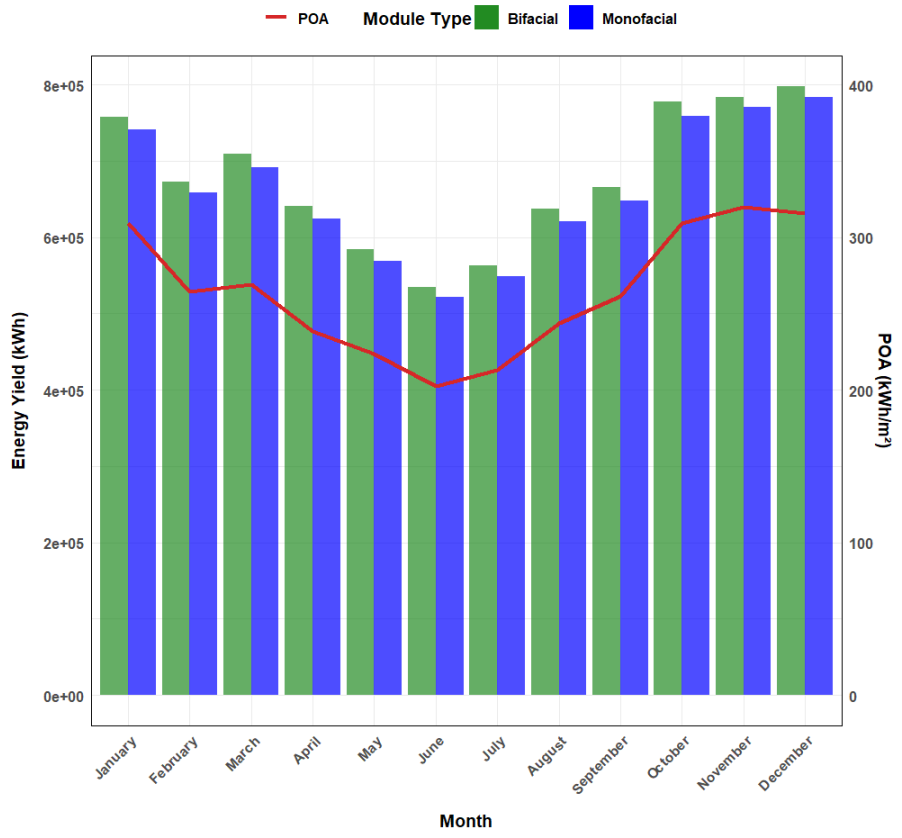

(b)

Figure 4.8: PV System Energy Yield & POA. Image (a) shows the relationship between the fixed-tilt monofacial & bifacial PV system's energy yield and irradiation. Image (b) shows the relationship between the single-axis tracking monofacial & bifacial PV system's energy yield and irradiation

The performance ratios of the systems are shown in Fig. 4.9. The single-axis tracking monofacial system has an average performance ratio (PR) of 0.81, while the single-axis tracking bifacial system has a PR of 0.83. The fixed-tilt monofacial system has a PR of 0.82, and the fixed-tilt bifacial system has a PR of 0.86.

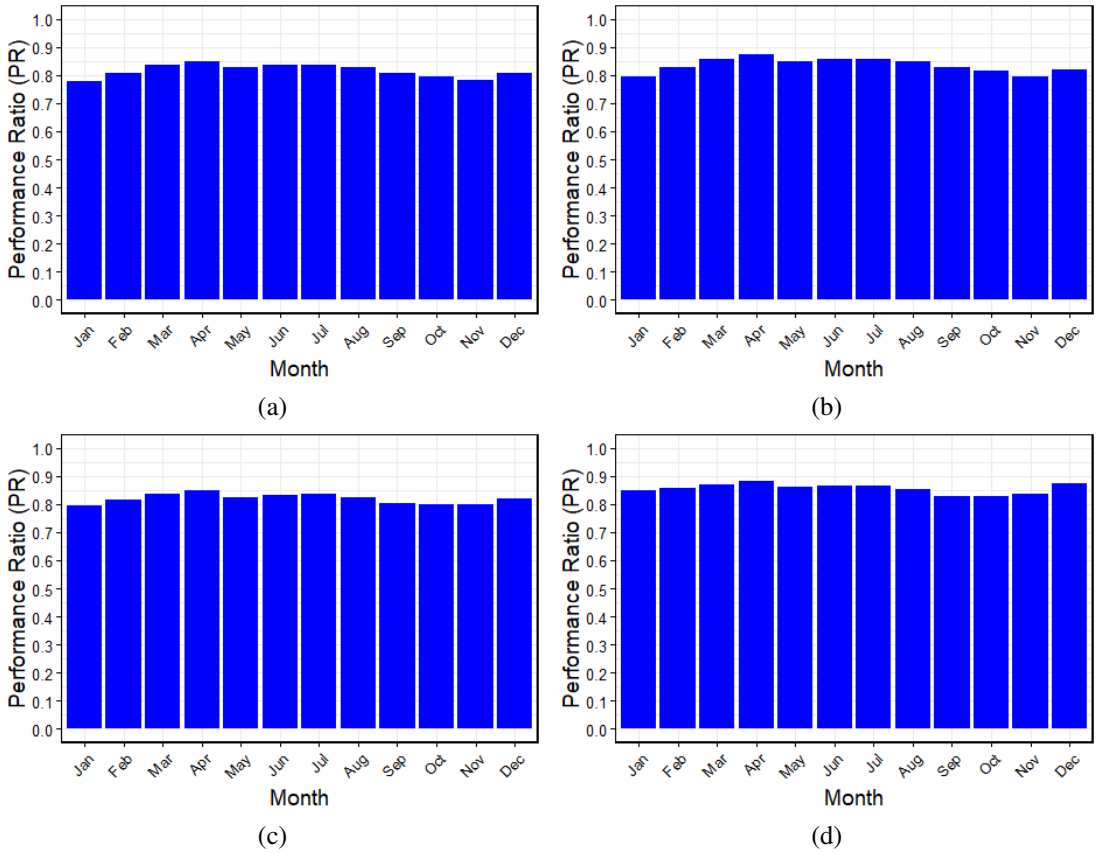

Figure 4.9: PV System Performance Ratios (PR). Image (a) shows the performance ratio (PR) of the single-axis tracking monofacial system. Image (b) shows the performance ratio (R) of the single-axis tracking bifacial system. Image (c) shows the performance ratio (PR) of the fixed-tilt monofacial system. Image (d) shows the performance ratio (PR) of the fixed-tilt bifacial system.

The losses in each system, calculated by the software, are shown step by step in Figs. 4.10, 4.11, 4.12, and 4.13. Single-axis tracking systems collect an additional 33.2% energy (3170.16 kWh/m²/year) through sun-tracking, while fixed-tilt systems tilted towards the north collect an additional 8.4% energy (2579.92.7 $\mathrm{kWh/m^2/year}$) compared to the GHI. This energy is the global incident irradiance in the collector

plane. The system then undergoes losses due to near shadings, incidence angle modifier (IAM), and soiling. Additionally, bifacial modules experience extra losses due to factors such as view factor and shading on the rear side, despite the increased incident radiation from ground reflection.

The final effective irradiation on collectors, after accounting for these losses and energy gains, is 2359 $kWh/m^2/year$ for the single-axis tracking monofacial system, 2952 $kWh/m^2/year$ for the single-axis tracking bifacial system, 2359 $kWh/m^2/year$ for the fixed-tilt monofacial system, and 2349 $kWh/m^2/year$ for the fixed-tilt bifacial system. This effective irradiation is multiplied by the total collector area for the respective systems to get the total luminous energy available on the collectors. The total luminous energy is multiplied by the efficiency at STC to get the array nominal energy of 9026718 kWh for the single-axis tracking monofacial system, 9336730 kWh for the single-axis tracking bifacial system, 7297326 kWh for the fixed-tilt monofacial system, and 7800941 kWh for the fixed-tilt bifacial system. The PV loss due to irradiance level and temperature is because PV modules do not work at STC. Other array losses such as the ohmic wiring losses, mismatch losses between strings and modules, and module quality decrease the array power further leading to the array virtual energy at MPP. This is the total energy from the full array, available at the inverter input. The systems then undergo inverter losses. The inverters were slightly undersized, resulting in some power loss due to power clipping at the nominal power of the inverter for each system. System unavailability is also accounted for as an additional loss. The final energy injected into the grid after all these losses is 7961336 kWh for the single-axis tracking monofacial system, 8149390 kWh for the single-axis tracking bifacial system, 6525316 kWh for the fixed-tilt monofacial system, and 6814454 kWh for the fixed-tilt bifacial system.

Additionally, to get a more accurate energy production for the single-axis tracking systems, the self-consumption was deducted from the energy output of these systems. The self-consumption power of the system is 0.2% of the nominal power output per tracker. This amount totalled to 1822 kWh/month. Once all the losses have been analysed, the

total energy generated by the different systems was found to be: single-axis tracking monofacial PV system = 7,939,608.50 kWh/a, single-axis tracking bifacial PV system = 8,127,519.80 kWh/a, fixed-tilt monofacial PV system = 6,525,316 kWh/a, and the fixed-tilt bifacial PV system = 6,814,457 kWh/a.

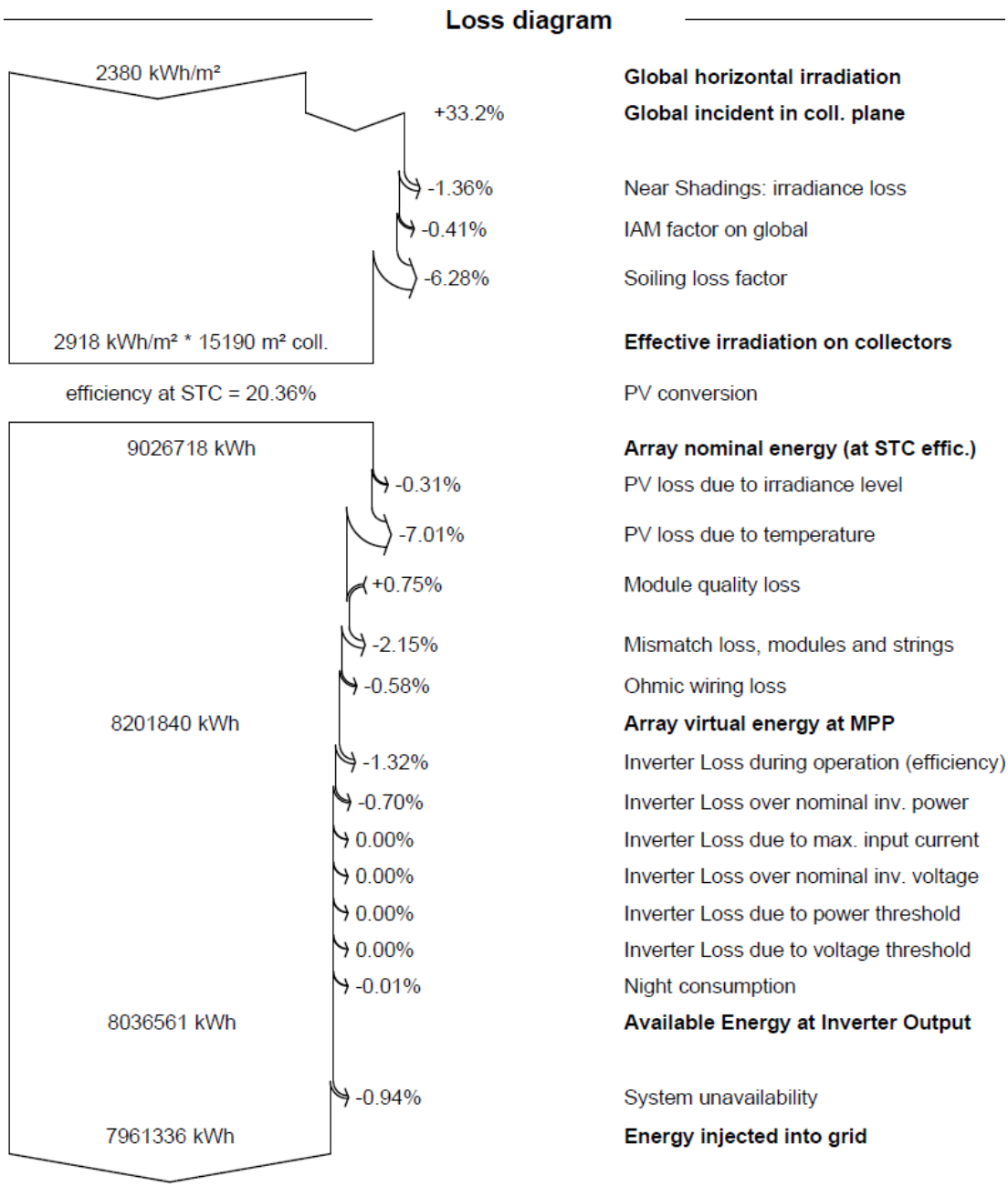

Figure 4.10: Single-Axis Tracking Monofacial System Loss Diagram

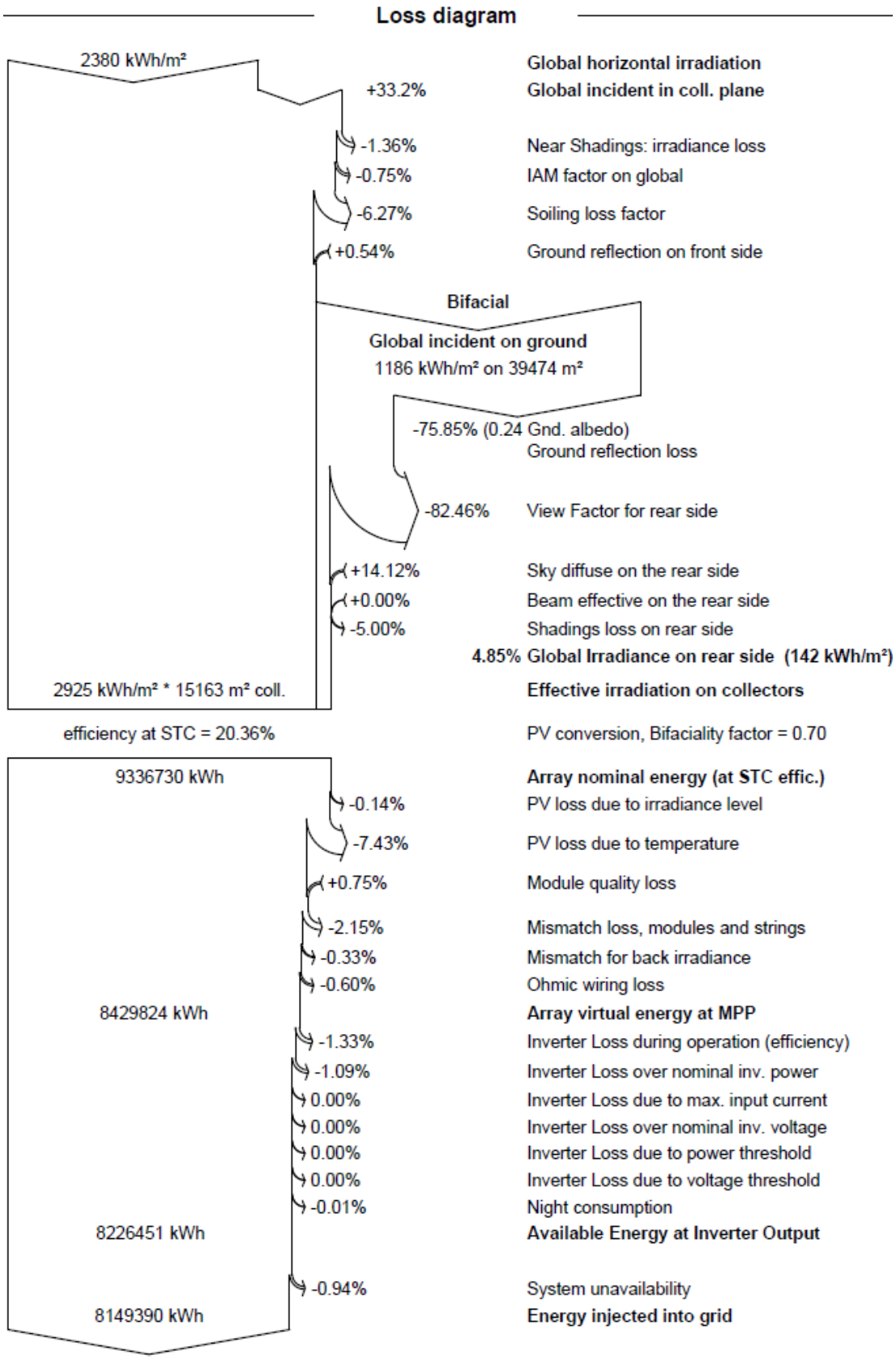

Figure 4.11: Single-Axis Tracking Bifacial System Loss Diagram

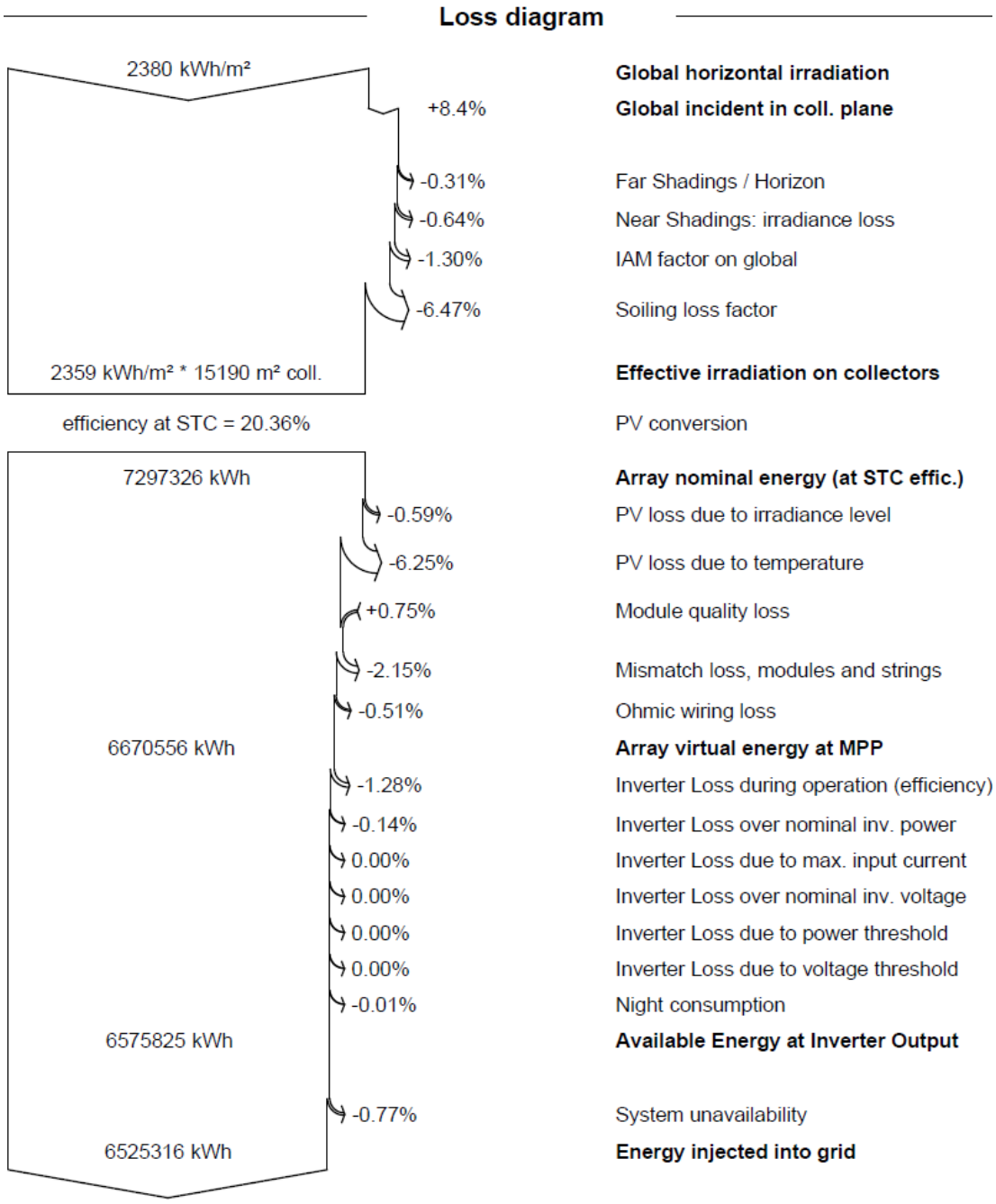

Figure 4.12: Fixed-Tilt Monofacial System Loss Diagram

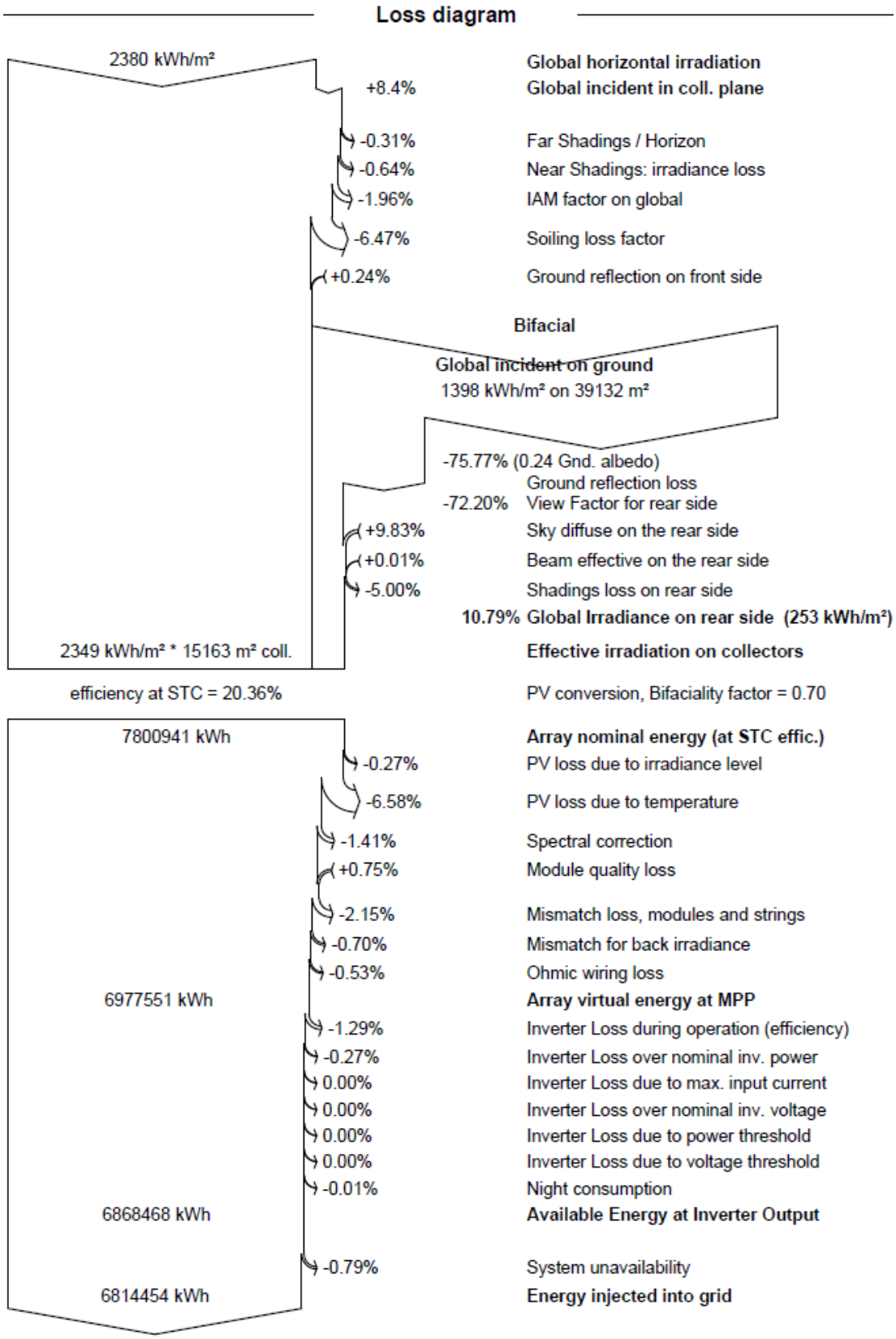

Figure 4.13: Fixed-Tilt Bifacial System Loss Diagram

The single-axis tracking bifacial PV system outperforms the single-axis tracking mono-facial PV system, in Fig. 4.14.

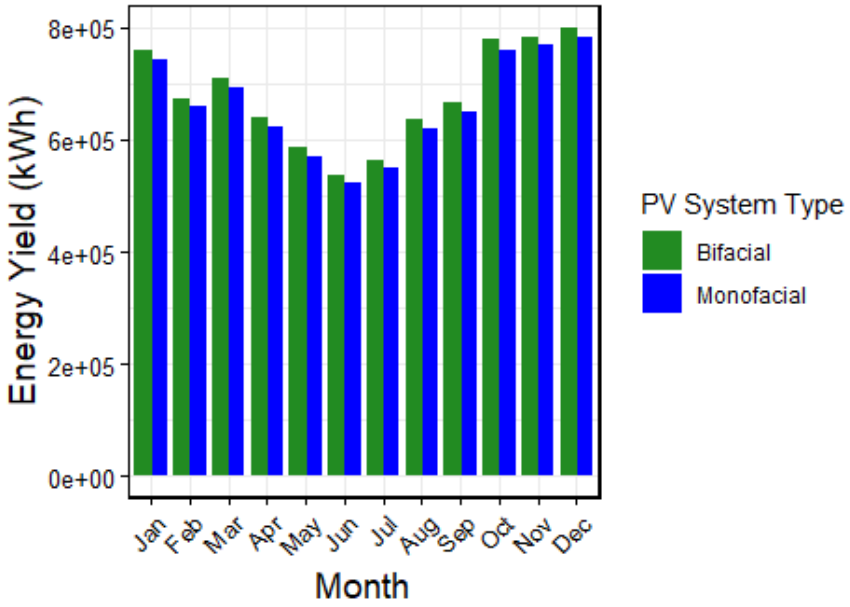

Figure 4.14: Single-Axis Tracking Energy Yield Comparison

The fixed-tilt bifacial PV system outperforms its monofacial counterpart in Fig. 4.15.

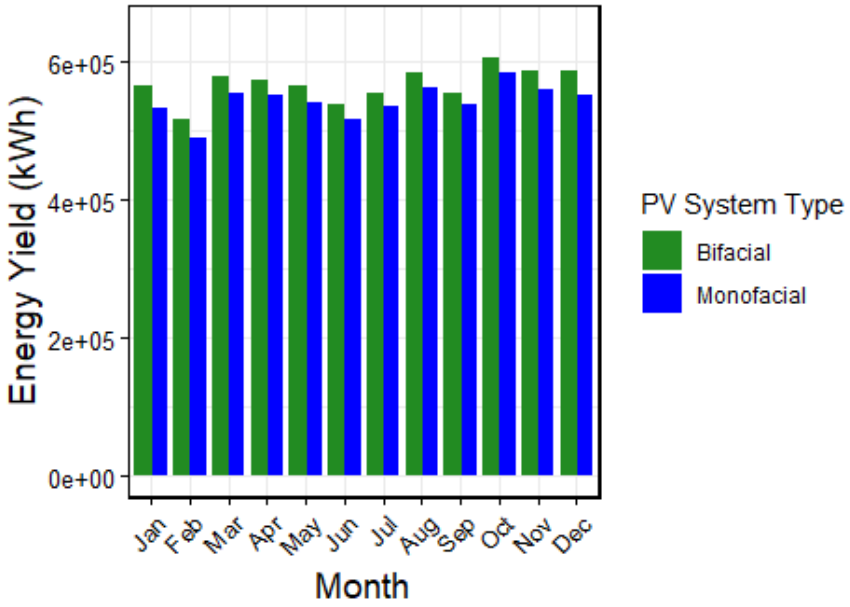

Figure 4.15: Fixed-Tilt Energy Yield Comparisons

A t-test was conducted to compare the means of energy yields between monofacial and bifacial configurations for both single-axis tracking and fixed-tilt PV systems.

In the single-axis tracking systems, the variances of energy production were calculated as 7,963,612,476 (Monofacial) and 8,085,211,229 (Bifacial), corresponding to standard deviations of 89 240 and 89 920, respectively. These variances are very close, indicating similar variability in energy output between the two systems. Despite

the slightly higher mean yield for bifacial systems (677,293 vs. 661,634), the difference was not statistically significant (t(22) = -0.4282, one-tail p = 0.3363; two-tail p = 0.6727). Both p-values exceed 0.05, supporting the conclusion that the observed difference in means is attributable to random variation rather than a systematic effect. In the fixed-tilt systems, the variances were 574,595,894 (Monofacial) and 579,697,848 (Bifacial), with standard deviations of 23,970 and 24,080, respectively. The near-identical variances reflect comparable spreads in energy production data. Here, the bifacial system's mean yield (567,871) was significantly higher than the monofacial system's mean (543,776). The t-statistic (t(22) = -2.4567) exceeded critical values for both one-tail (1.717) and two-tail (2.074) tests, with p-values (one-tail = 0.0111; two-tail = 0.0224) falling below 0.05. This robustly rejects the null hypothesis of equal means, confirming a statistically significant advantage for bifacial fixed-tilt systems. While variances and standard deviations were closely matched in both configurations, the fixed-tilt bifacial system demonstrated a statistically significant performance improvement over its monofacial counterpart. In contrast, single-axis tracking systems showed no such statistical significant difference, despite comparable data spreads.

4.2 Financial Assessment

4.2.1 Results for PV Systems

The cost estimations of the different systems are given in Table. 4.2 which were obtained from relevant local industry data to offer a comprehensive understanding of the financial landscape associated with installing PV systems of this capacity.

Table 4.2: Financial Parameters of the PV Systems

Parameter	1-Axis Tracking Monofacial	1-Axis Tracking Bifacial	Fixed-Tilt Monofacial	Fixed-Tilt Bifacial
CAPEX (N$)	45,889,947.54	48,564,586.58	41,771,866.07	44,446,505.11
OPEX (N$)	688,349.21	728,468.80	626,577.99	666,697.58

To calculate the discounted cash flow using Eq. (3.4), a degradation rate of 0.65% was used for monofacial modules and 1.2% for bifacial modules. The electricity tariff was set at N$ 2.12/kWh which was the price of electricity during the year the plant was commissioned [53]. The foreseeable increase in electricity was set to an average of

5.69% per year based on Nampower's historical electricity tariffs [54], calculated using Eq. (3.3). The CAPEX of the system will increase due to the inverter replacement expenditure approximately halfway through the system's lifetime. The discount rate used in the calculations is 10%, based on the fixed deposit rates from First National Bank (FNB) and Standard Bank's Capricorn Unit Trusts [55, 56].

Additionally, the historical inflation rate over the past 10 years was calculated to be 4.8%, with values provided by the World Bank [57]. This inflation rate was applied to the CAPEX and OPEX using Eq. (3.5) and the discounted OPEX and CAPEX were calculated using Eq. (3.11). The operational expenditure (OPEX) was assumed to be 1.5% of the CAPEX.

The LCOE was found using Eq. (2.6) for the different PV systems ranging from 0.85 to 1.00 N$/kWh. Single-axis tracking monofacial PV systems have the lowest LCOE, making them the most cost-effective option in terms of energy production costs. The payback period, found using Eq. (2.7), varies slightly among the systems, with single-axis tracking monofacial PV systems having the shortest payback period of 3 years, 2 months. This indicates a quicker return on investment compared to other systems. The IRR ranges from 31.50% to 35.60%. Single-axis tracking monofacial systems again show the highest IRR, suggesting they are the most financially beneficial. While bifacial systems generally have higher LCOE and longer payback periods compared to monofacial systems, they still offer competitive IRR. The financial performance indicators for the four systems in this study are summarised in Table 4.3.

Table 4.3: A comparison of the financial performance of the PV systems

Type of System	Module Technology	LCOE (N$/kWh)	Payback Period (years)	IRR (%)
Single-Axis Tracking	Monofacial	0.85	3.11	35.60
Single-Axis Tracking	Bifacial	0.91	3.27	32.50
Fixed-tilt	Monofacial	0.94	3.45	32.00
Fixed-tilt	Bifacial	1.00	3.62	31.50

The relationship between the discount rate and NPV can be seen in Fig. 4.16 and Fig. 4.17. The discount rate helps assess whether the project will generate sufficient returns to justify the investment. A higher cost of capital a project can sustain while remaining viable is equal to its IRR so selecting a discount rate above the IRR can lead to a negative NPV, indicating the project is not worth the financial investment. The single-axis tracking monofacial system had the highest IRR out of the 4 systems. The discount rate at which the net present value is equal to zero is known as the IRR.

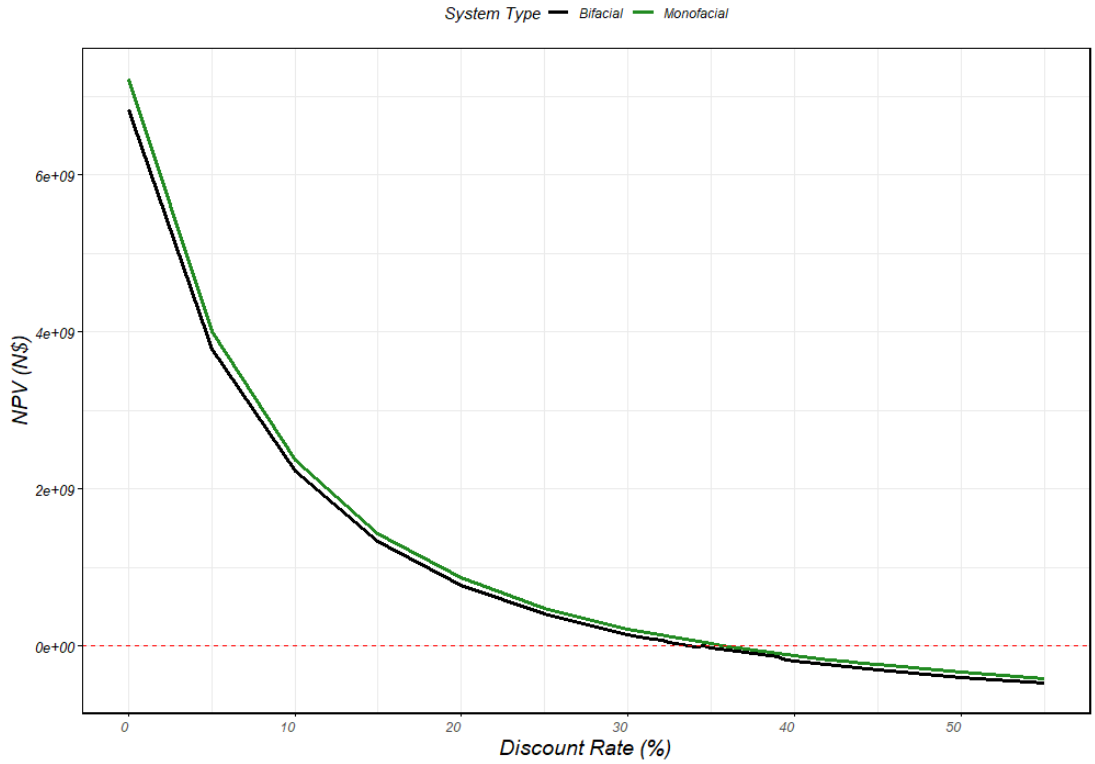

Figure 4.16: Single- Axis Tracking PV System's NPV vs Discount Rate. The single-axis tracking monofacial and bifacial PV system net present value at different discount rate.

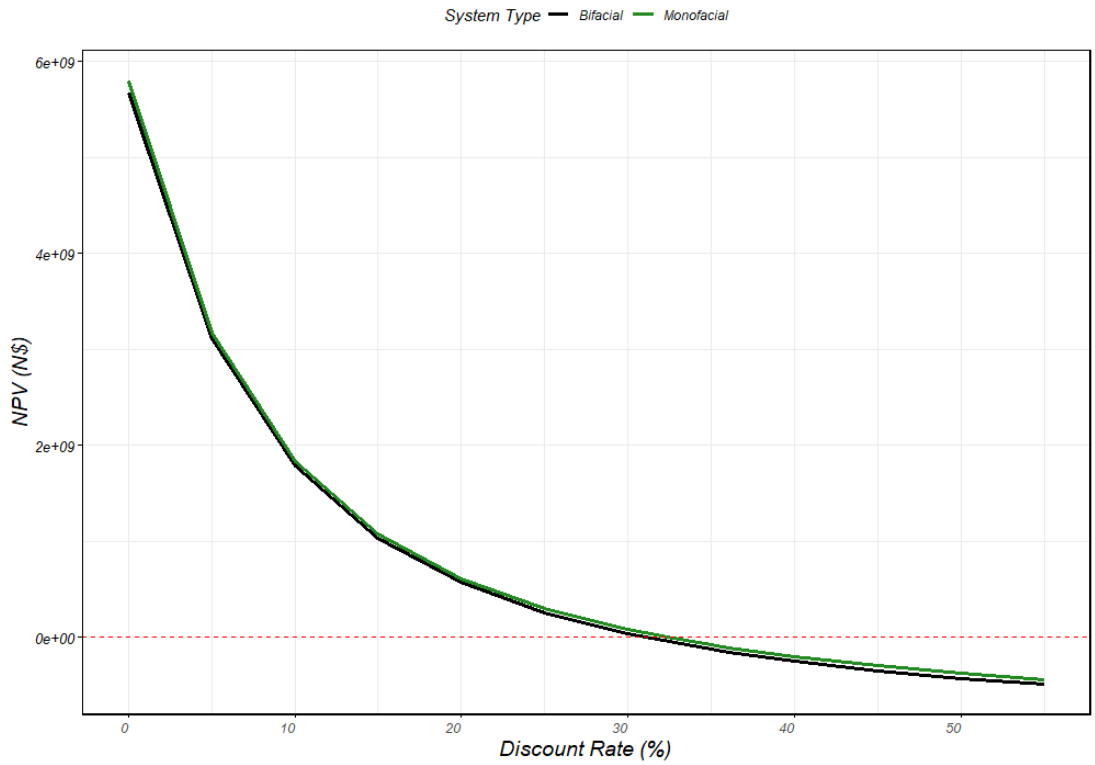

Figure 4.17: Fixed-Tilt PV System's PV System's NPV vs Discount Rate. Fixed-tilt monofacial and bifacial PV system net present value at different discount rates.

The discounted NPV of the systems after 25 years are N$ 185 245 609.58 for the single-axis tracking monofacial system, N$ 173 785 499.30 for the single-axis tracking bifacial system, N$ 147 422 689.34 for the fixed-tilt monofacial system, and N$ 140 782 691.28 for the fixed-tilt bifacial system.

All four systems achieve break-even within 3–4 years, as their cumulative net cash flows turn positive during this period as seen in Fig. 4.18. However, the single-axis tracking monofacial system breaks even fastest, followed by the single-axis tracking bifacial system, the fixed-tilt monofacial system, and finally the fixed-tilt bifacial system, which takes the longest. The fixed-tilt bifacial system has the longest break-even time due to its higher installation and maintenance costs, combined with lower energy yields compared to single-axis tracking systems.

Systems like the single-axis tracking monofacial or fixed-tilt monofacial recover costs faster, making them ideal for businesses prioritising short-term returns or working with limited budgets. In contrast, bifacial systems (both single-axis tracking and fixed-tilt) require higher upfront investment but generate more energy over their lifespan, mak-

ing them better suited for long-term projects. While the single-axis tracking bifacial system's slower payback may deter some businesses, its superior energy production offers long-term benefits. The fixed-tilt bifacial system, however, remains financially challenging unless costs decrease.

Overall, the single-axis tracking monofacial system outperforms others across metrics like cost recovery and simplicity, closely followed by the single-axis tracking bifacial system.

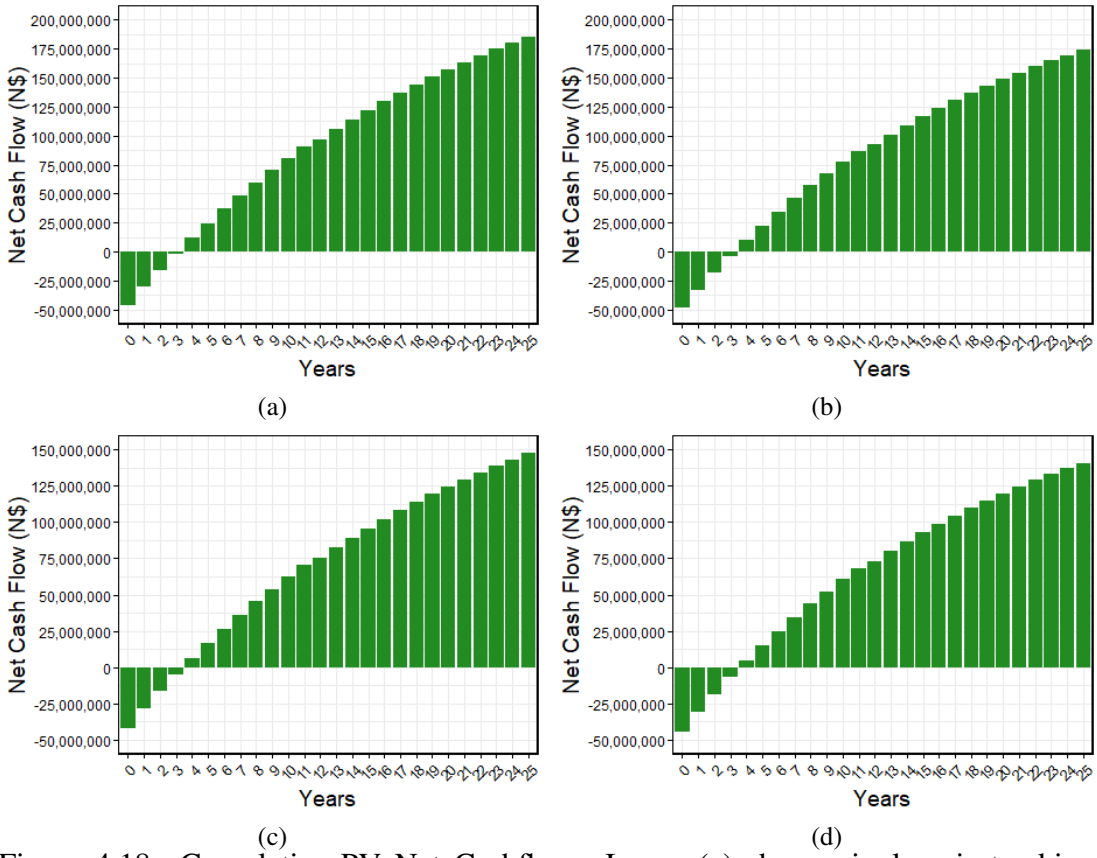

Figure 4.18: Cumulative PV Net Cashflow. Image (a) shows single-axis tracking monofacial cumulative present value net cashflow. Image (b) shows single-axis tracking bifacial cumulative PV net cashflow. Image (c) shows fixed-tilt monofacial cumulative present value net cashflow. Image (d) shows fixed-tilt bifacial cumulative PV net cashflow

Chapter 5

Conclusion and Recommendations

This chapter synthesises findings, concluding that single-axis tracking monofacial systems offer optimal financial feasibility in Windhoek. It highlights contributions to localized PV system design and discusses limitations and recommendations.

5.1 Conclusion

The comprehensive evaluation of the bifacial and monofacial single-axis tracking and fixed-tilt systems, including performance assessments and rigorous financial analysis, indicated that the optimal system to efficiently meet the business's energy demands while providing a cost-effective installation solution is the 3MW single-axis tracking monofacial PV system.

The performance yield assessment showed that the single-axis tracking bifacial system had the highest energy yield production of 8,127,519.80 kWh/a among all four systems which is beneficial for maximising energy production. However, there was no statistical significance between the energy yield of this system and the single-axis tracking monofacial PV system, which had an energy production yield of 7,939,608.50 kWh/a.

Based on financial evaluations of all four systems, the most cost-effective solution capable of meeting a portion of the business's energy demands was the single-axis tracking monofacial PV system. This system had the lowest LCOE of N$0.85/kWh, while the fixed-tilt bifacial PV system had the highest LCOE of N$1.00/kWh. Additionally, the single-axis tracking monofacial PV system had the shortest payback period of 3 years, 2 months and the highest IRR of 35.62%, meaning it would recover its investment the fastest and provide the best financial returns among the four systems.
Under Windhoek conditions, bifacial PV systems do not outperform monofacial PV systems. Bifacial systems have higher LCOEs, longer payback periods, and lower IRRs than monofacial systems.

5.2 Recommendations

The optimal PV system for Windhoek's conditions is the single-axis tracking system with monofacial modules. This design offers the quickest return on investment and the lowest levelized cost of electricity (LCOE). Therefore, businesses in the Windhoek area are advised to adopt single-axis tracking systems with monofacial modules to maximise efficiency and financial returns. To enhance the accuracy of simulations, it is recommended to measure the albedo on-site, as real-time albedo data is currently unavailable. This will allow for a more precise comparison of performance.

Bibliography

[1] World Bank Group 2024 Global solar atlas accessed: 2024-03-25 URL https://globalsolaratlas.info/map?c=-22.633025,16.498718,9&s=-22.57761,17.077274&m=site

[2] Atonometrics What is a PV Module IV Curve? accessed: 12-02-2023 URL https://www.atonometrics.com/applications/what-is-a-pv-module-iv-curve/

[3] Fertig F, Nold S, Wöhrle N, Greulich J, Hädrich I, Krauß K, Mittag M, Biro D, Rein S and Preu R 2016 *Progress in photovoltaics: research and applications* **24** 800–817

[4] Duran C, Hering P, Buck T and Peter K 2011 Characterization of bifacial silicon solar cells and modules: A New Step *European Photovoltaic Solar Energy Conference*

[5] Kopecek R and Libal J 2021 *Energies* **14** 2076

[6] International Energy Agency 2021 Solar Photovoltaic (PV) Tech. rep. IEA URL https://www.iea.org/reports/solar-photovoltaic

[7] International Renewable Energy Agency 2020 Renewable Power Generation Costs in 2019 Tech. rep. IRENA accessed: 30-07-2023 URL https://www.irena.org/-/media/Files/IRENA/Agency/Publication/2020/Jun/IRENA_Renewable-Power-Generation-Costs-2019.pdf

[8] Electricity Control Board 2023 *SAPP AND MSB MARKET ACCESS GUIDE* (Electricity Control Board) accessed: 15-09-2023 URL https://www.ecb.org.na/wp-content/uploads/2023/08/SAPP_MSB_Market_Access_Guide.pdf

[9] Bluestem Energy Solutions 2024 Bifacial Versus Monofacial Solar Panels: An Analysis accessed: 10-12-2023 URL https://www.bluestemenergysolutions.com/bifacial-versus-monofacial-solar-panels-an-analysis/

[10] Solar Power World 2017 Specific Yield Overview accessed: 2023-04-19 URL https://www.solarpowerworldmisc.com/2017/08/specific-yield-overview/

[11] LG Electronics 2017 *Bifacial Design Guide (Full Version)* accessed: 21-08-2023 URL https://www.lg.com/global/business/download/resources/solar/Bifacial_design_guide_Full_ver.pdf

[12] Zhang X, Monokroussos C, Schweiger M and Heinze M 2023 *Photovoltaics International* **11**

[13] Lamers M, Özkalay E, Gali R, Janssen G, Weeber A, Romijn I and Van Aken B 2018 *Solar Energy Materials and Solar Cells* **185** 192–197

[14] McIntosh K, Abbott M, Sudbury B and Meydbray J 2019 *IEEE Journal of Photovoltaics* **9** 1504–1512

[15] Rossa C, Martínez-Moreno F, Francisco and Lorenzo E 2021 *Progress in Photovoltaics: Research and Applications* **29** 1223–1235

[16] Raina G and Sinha S 2021 *Materials Today: Proceedings* **46** 5242–5247

[17] Mesquita D, Silva J, Moreira H, Kitayama M and Villalva M 2019 A review and analysis of technologies applied in PV modules *2019 IEEE PES Innovative Smart Grid Technologies Conference-Latin America (ISGT Latin America)* (IEEE) pp 1–6

[18] Smith B, Woodhouse M, Horowitz K, Silverman T, Zuboy J and Margolis R 2021 Photovoltaic (PV) module technologies: 2020 benchmark costs and technology evolution framework results Tech. rep. National Renewable Energy Lab.(NREL), Golden, CO (United States)

[19] Bhang B, Lee W, Kim G, Choi J, Park S and Ahn H K 2019 *IEEE Journal of Photovoltaics* **9** 1413–1420

[20] Song Z, Li C, Chen L and Yan Y 2022 *Advanced materials* **34** 2106805

[21] PV Education 2023 Solar Cell IV Curve accessed: 11-09-2023 URL `https://www.pveducation.org/pvcdrom/solar-cell-operation/iv-curve`

[22] PV Education 2023 Solar Cell Efficiency accessed: 05-10-2023 URL `https://www.pveducation.org/pvcdrom/solar-cell-operation/solar-cell-efficiency`

[23] PVsyst 2023 Bifacial Systems accessed: 15-04-2023 URL `https://www.pvsyst.com/help/bifacial_systems.htm`

[24] Fertig F, Wöhrle N, Greulich J, Krauß K, Lohmüller E, Meier S, Wolf A and Rein S 2016 *Progess in Photovoltaics: Research and Applications.* **24** 818–829

[25] Wöhrle N, Fellmeth T, Greulich J, Bitnar B, Neuhaus H, Palinginis P, Köhler R and Rein S 2017 *Energy Procedia* **124** 225–234

[26] Duran C, Deuser H, Harney R and Buck T 2011 *Energy Procedia* **8** 88–93

[27] National Renewable Energy Laboratory (NREL) 2021 Bifacial Solar Photovoltaic Modules: Opportunities and Challenges accessed: 05-04-2024 URL https://www.nrel.gov/docs/fy21osti/80281.pdf

[28] Liang T, Pravettoni M, Deline C, Stein J, Kopecek R, Singh P, Luo W, Wang Y, Aberle A and Khoo S 2019 *Energy & Environmental Science* **12** 116–148

[29] Jouttijärvi S, Lobaccaro G, Kamppinen A and Miettunen K 2022 *Renewable and Sustainable Energy Reviews* **161** 112354

[30] Leonardi M, Corso R, Milazzo R G, Connelli C, Foti M, Gerardi C, Bizzarri F, Privitera S M and Lombardo S A 2021 *Energies*

[31] Hutchins M 2020 Temperature and the Case for Bifacial accessed: 17-09-2023 URL https://www.pv-magazine.com/2020/07/28/temperature-and-the-case-for-bifacial/

[32] for Solar Energy Systems F I 2024 Photovoltaics Report Tech. rep. Fraunhofer accessed: 2023-11-20 URL https://www.ise.fraunhofer.de/content/dam/ise/de/documents/publications/studies/Photovoltaics-Report.pdf

[33] Chudinzow D, Klenk M and Eltrop L 2020 *Solar Energy* **207** 564–578

[34] Pelaez S, Kostuk R, Deline C, Greenberg P and Stein J 2018 Model and Validation of Single-Axis Tracking with Bifacial Photovoltaics: Preprint Tech. rep. NREL nREL/CP-5K00-72039 URL https://www.nrel.gov/docs/fy19osti/72039.pdf

[35] Janssen G, Burgers A, Binani A, Carr A, Aken B V, Romijn I, Klenk M, Nussbaumer H and Baumann T 2018 How to maximize the kWh/kWp ratio: simulations of single-axis tracking in bifacial systems *35th European Photovoltaic Solar Energy Conference and Exhibition, EU PVSEC* pp 1573–1577

[36] Urs R, Sadiq M, Mayyas A and Sumaiti A 2023 *International Journal of Energy Research* **2023** 1612600

[37] Khalid A, Mitra I, Warmuth W and Schacht V 2016 *Renewable and Sustainable Energy Reviews* **65** 1139–1158 ISSN 1364-0321

[38] PVsyst SA Unavailability Loss accessed: 02-11-2023 URL https://www.pvsyst.com/help/unavailability_loss.html

[39] Hayes M, Mundy D, Samal A and Drijber R 2016 Photovoltaic Solar Energy: Development and Current Research accessed: 20-11-01 URL https://extensionpubs.unl.edu/publication/ec3008/pdf/view/ec3008-2016.pdf

[40] Fouad M, Shihata L and Morgan E 2017 *Renewable and Sustainable Energy Reviews* **80** 1499–1511

[41] Guo B, Javed W, Figgis B and Mirza T 2015 Effect of dust and weather conditions on photovoltaic performance in Doha, Qatar *2015 First Workshop on Smart Grid and Renewable Energy (SGRE)* (IEEE) pp 1–6

[42] Maghami M, Hizam H, Gomes C, Radzi A, Rezadad I and Hajighorbani S 2016 *Renewable and Sustainable Energy Reviews* **59** 1307–1316

[43] Stanka N, Aboltins A and Palabinskis J 2020 Impact of high temperature and other factors on PV module efficiency on small farms in Latvia *19th International Scientific Conference Engineering for Rural Development Proceedings. Jelgava* vol 19 pp 472–480

[44] DNV Bifacial PV Technology: Technical Considerations accessed:20-06-2023 URL https://www.dnv.com/article/bifacial-pv-technology-technical-considerations186095/#:~:text=The%20yield%20from%20a%20bifacial,temperature%2C%20wind%20speed%2C%20albedo%2C

[45] Helioscope Modeling 101 accessed:15-03-2023 URL availableat{https://help-center.helioscope.com/hc/en-us/articles/13804165205395-Modeling-101}

[46] NASA Langley Research Center Albedo Values accessed: 2023-04-17 URL https://mynasadata.larc.nasa.gov/basic-page/albedo-values#:~:text=A%20surface%20with%20a%20high,urban%20surfaces%2C%20such%20as%20asphalt.

[47] da Fonseca J, de Oliveira F, Prieb C and Krenzinger A 2020 *Solar Energy* **196** 196–206

[48] Annigoni E, Virtuani A, Caccivio M, Friesen G, Chianese D and Ballif C 2019 *Progress in Photovoltaics: Research and Applications* **27** 760–778

[49] National Renewable Energy Laboratory 2022 Measuring and Modeling Bifacial Technologies accessed: 12-08-2023 URL https://www.nrel.gov/docs/fy22osti/82540.pdf

[50] Rodríguez-Gallegos C, Bieri M, Gandhi O, Singh J, Reindl T and Panda S 2018 *Solar Energy*

[51] Mermoud A and Wittmer B 2018 *Proceedings of the EUPVSEC, Brussels, Belgium* 7–11

[52] Clifford M B G and King D 2018 *IEEE Journal of Photovoltaics* **8** 1651–1656 explicit equation for soiling loss using $P_{\max}$ notation.

[53] Republic of Namibia 2022 Namibia Government Gazette, No. 7929, Dated 2022-10-14 accessed: 2023-05-09 URL https://archive.gazettes.africa/archive/na/2022/na-government-gazette-dated-2022-10-14-no-7929.pdf

[54] NamPower 2022 NamPower Distribution Tariff 2022-2023 accessed: 2023-05-09 URL https://www.nampower.com.na/public/docs/tariffs/Distribution%20Tariff%202022-2023.pdf

[55] Namibia F 2023 Fixed Deposit - First National Bank Namibia accessed: 2023-05-01 URL https://www.misc.fnbnamibia.com.na/invest/fixed-deposit.html

[56] Namibia C 2023 Unit Trusts - CAM Namibia accessed: 2023-10-01 URL https://www.cam.com.na/Pages/Unit-Trusts.aspx

[57] World Bank 2024 Namibia — Data accessed: 2023-10-01 URL https://data.worldbank.org/country/namibia

Appendix

A.1 Datasheets

A.1.1 Bifacial Module Datasheet

www.jinkosolar.com

Solar JinKO
Building Your Trust in Solar

Tiger Pro 72HC-BDVP

525-545 Watt

BIFACIAL MODULE WITH DUAL GLASS

P-Type

Positive power tolerance of 0~+3%

IEC61215(2016), IEC61730(2016)

ISO9001:2015: Quality Management System

ISO14001:2015: Environment Management System

ISO45001:2018
Occupational health and safety management systems

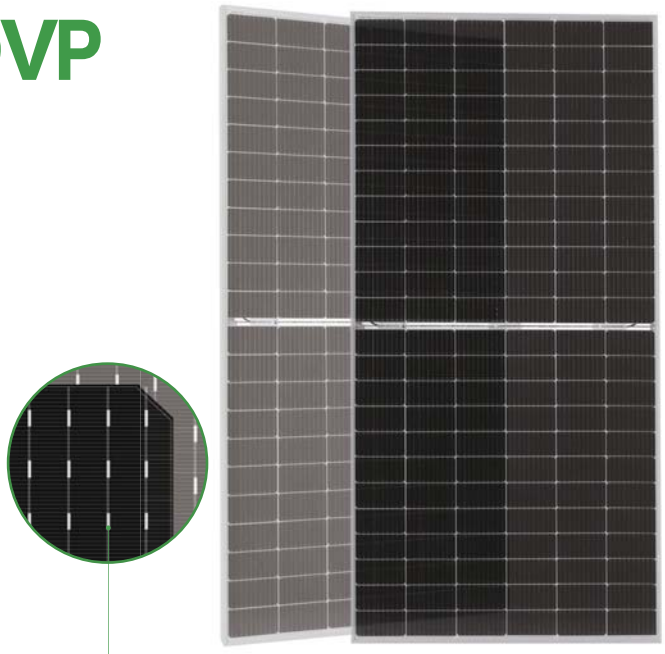

Bifacial Technology

Key Features

Multi Busbar Technology
Better light trapping and current collection to improve module power output and reliability.

Longer Life-time Power Yield
0.45% annual power degradation and 30 year linear power warranty.

PID Resistance
Excellent Anti-PID performance guarantee via optimized mass-production process and materials control.

Enhanced Mechanical Load
Certified to withstand: wind load (2400 Pascal) and snow load (5400 Pascal).

Higher Power Output
Module power increases 5-25% generally, bringing significantly lower LCOE and higher IRR.

LINEAR PERFORMANCE WARRANTY

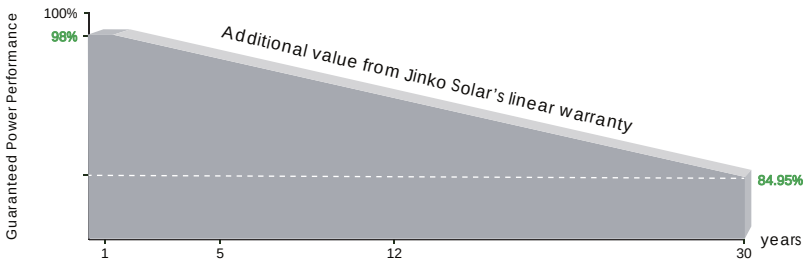

12 Year Product Warranty

30 Year Linear Power Warranty

0.45% Annual Degradation Over 30 years

Engineering Drawings

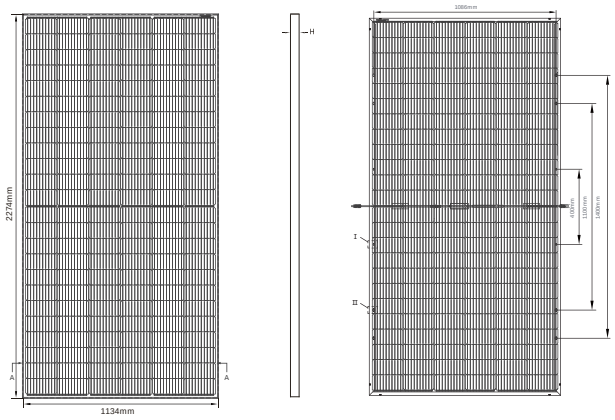

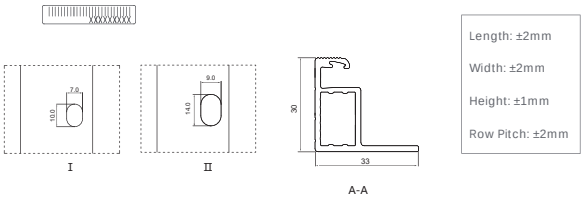

Length: ±2mm
Width: ±2mm
Height: ±1mm
Row Pitch: ±2mm

Packaging Configuration

(Two pallets = One stack)

35pcs/pallets, 70pcs/stack, 630pcs/ 40'HQ Container

Electrical Performance & Temperature Dependence

Current-Voltage & Power-Voltage Curves (535W)

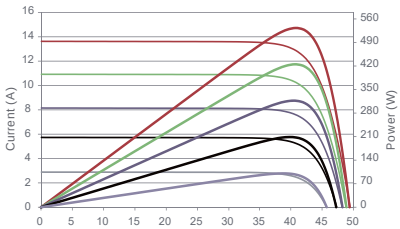

Temperature Dependence of Isc,Voc,Pmax

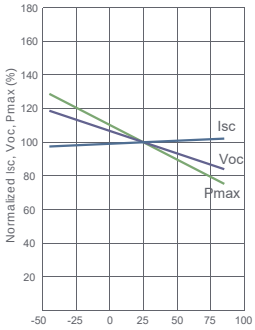

Mechanical Characteristics

Cell Type	P type Mono-crystalline
No. of cells	144 (6×24)
Dimensions	2274×1134×30mm (89.53×44.65×1.18 inch)
Weight	34.3 kg (75.6 lbs)
Front Glass	2.0mm, Anti-Reflection Coating
Back Glass	2.0mm, Anti-Reflection Coating
Frame	Anodized Aluminium Alloy
Junction Box	IP68 Rated
Output Cables	TUV 1×4.0mm² (+): 400mm , (-): 200mm or Customized Length

SPECIFICATIONS

Module Type	JKM525M-72HL4-BDVP		JKM530M-72HL4-BDVP		JKM535M-72HL4-BDVP		JKM540M-72HL4-BDVP		JKM545M-72HL4-BDVP	
	STC	NOCT	STC	NOCT	STC	NOCT	STC	NOCT	STC	NOCT
Maximum Power (Pmax)	525Wp	391Wp	530Wp	394Wp	535Wp	398Wp	540Wp	402Wp	545Wp	405Wp
Maximum Power Voltage (Vmp)	40.80V	37.81V	40.87V	37.88V	40.94V	37.94V	41.13V	38.08V	41.32V	38.25V
Maximum Power Current (Imp)	12.87A	10.33A	12.97A	10.41A	13.07A	10.49A	13.13A	10.55A	13.19A	10.60A
Open-circuit Voltage (Voc)	49.42V	46.65V	49.48V	46.70V	49.54V	46.76V	49.73V	46.94V	49.92V	47.12V
Short-circuit Current (Isc)	13.63A	11.01A	13.73A	11.09A	13.83A	11.17A	13.89A	11.22A	13.95A	11.27A
Module Efficiency STC (%)	20.36%		20.55%		20.75%		20.94%		21.13%	
Operating Temperature(℃)	-40℃~+85℃									
Maximum system voltage	1500VDC (IEC)									
Maximum series fuse rating	30A									
Power tolerance	0~+3%									
Temperature coefficients of Pmax	-0.35%/℃									
Temperature coefficients of Voc	-0.28%/℃									
Temperature coefficients of Isc	0.048%/℃									
Nominal operating cell temperature (NOCT)	45±2℃									
Refer. Bifacial Factor	70±5%									

BIFACIAL OUTPUT-REARSIDE POWER GAIN

5%	Maximum Power (Pmax)	551Wp	557Wp	562Wp	567Wp	572Wp
	Module Efficiency STC (%)	21.38%	21.58%	21.78%	21.99%	22.19%
15%	Maximum Power (Pmax)	604Wp	610Wp	615Wp	621Wp	623Wp
	Module Efficiency STC (%)	23.41%	23.64%	23.86%	24.08%	24.30%
25%	Maximum Power (Pmax)	656Wp	663Wp	669Wp	675Wp	681Wp
	Module Efficiency STC (%)	25.45%	25.69%	25.93%	26.18%	26.42%

*STC: Irradiance 1000W/m² Cell Temperature 25°C AM=1.5

NOCT: Irradiance 800W/m² Ambient Temperature 20°C AM=1.5 Wind Speed 1m/s

A.1.2 Monofacial Module Datasheet

Harvest the Sunshine

DEEP BLUE 3.0

Mono

550W MBB Half-cell Module
JAM72S30 525-550/MR Series

Introduction

Assembled with 11BB PERC cells, the half-cell configuration of the modules offers the advantages of higher power output, better temperature-dependent performance, reduced shading effect on the energy generation, lower risk of hot spot, as well as enhanced tolerance for mechanical loading.

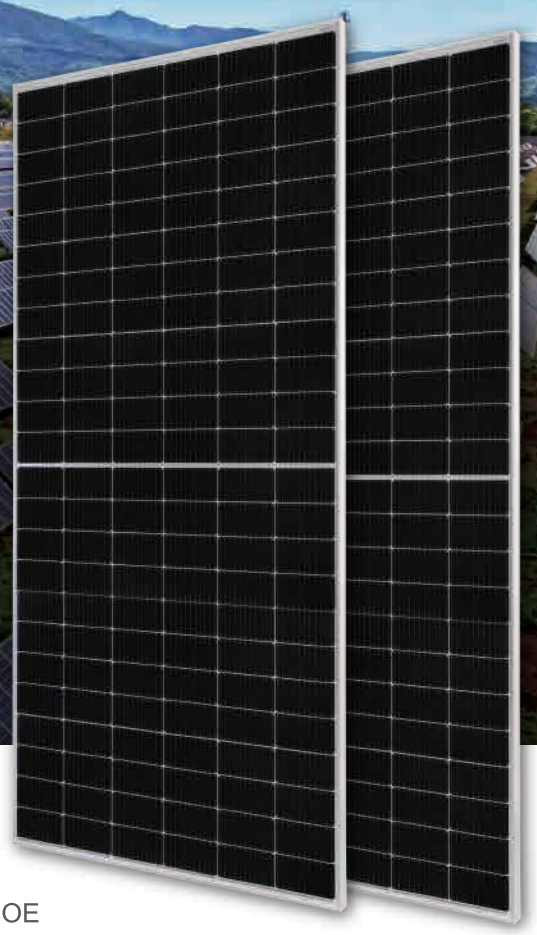

- Higher output power
- Lower LCOE
- Less shading and lower resistive loss
- Better mechanical loading tolerance

Superior Warranty

- 12-year product warranty
- 25-year linear power output warranty

0.55% Annual Degradation Over 25 years

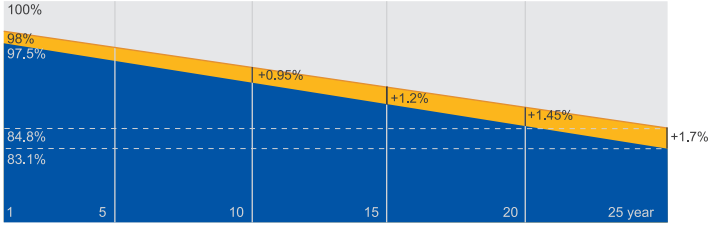

New linear power warranty Standard module linear power warranty

Comprehensive Certificates

- IEC 61215, IEC 61730,UL 61215, UL 61730
- ISO 9001: 2015 Quality management systems
- ISO 14001: 2015 Environmental management systems
- ISO 45001: 2018 Occupational health and safety management systems
- IEC TS 62941: 2016 Terrestrial photovoltaic (PV) modules – Guidelines for increased confidence in PV module design qualification and type approval

JA SOLAR

www.jasolar.com

JA SOLAR

JAM72S30 525-550/MR Series

MECHANICAL DIAGRAMS

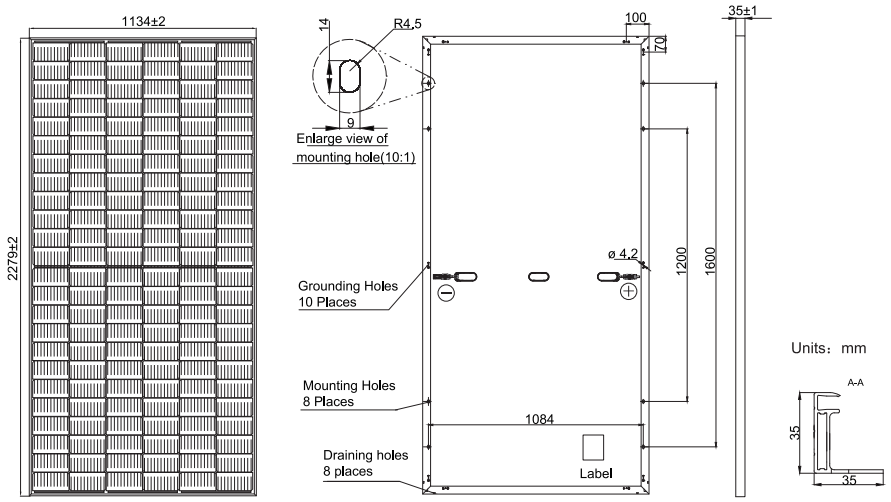

Remark: customized frame color and cable length available upon request

SPECIFICATIONS

Cell	Mono
Weight	28.6kg±3%
Dimensions	2279±2mm×1134±2mm×35±1mm
Cable Cross Section Size	4mm²（IEC），12 AWG(UL)
No. of cells	144(6×24)
Junction Box	IP68, 3 diodes
Connector	QC 4.10(1000V) QC 4.10-35(1500V)
Cable Length (Including Connector)	Portrait: 300mm(+)/400mm(-); Landscape: 1300mm(+)/1300mm(-)
Packaging Configuration	31pcs/Pallet, 620pcs/40ft Container

ELECTRICAL PARAMETERS AT STC

TYPE	JAM72S30 -525/MR	JAM72S30 -530/MR	JAM72S30 -535/MR	JAM72S30 -540/MR	JAM72S30 -545/MR	JAM72S30 -550/MR
Rated Maximum Power(Pmax) [W]	525	530	535	540	545	550
Open Circuit Voltage(Voc) [V]	49.15	49.30	49.45	49.60	49.75	49.90
Maximum Power Voltage(Vmp) [V]	41.15	41.31	41.47	41.64	41.80	41.96
Short Circuit Current(Isc) [A]	13.65	13.72	13.79	13.86	13.93	14.00
Maximum Power Current(Imp) [A]	12.76	12.83	12.90	12.97	13.04	13.11
Module Efficiency [%]	20.3	20.5	20.7	20.9	21.1	21.3
Power Tolerance	0~+5W					
Temperature Coefficient of Isc(α_Isc)	+0.045%°C					
Temperature Coefficient of Voc(β_Voc)	-0.275%/°C					
Temperature Coefficient of Pmax(γ_Pmp)	-0.350%/°C					
STC	Irradiance 1000W/m², cell temperature 25°C, AM1.5G					

Remark: Electrical data in this catalog do not refer to a single module and they are not part of the offer.They only serve for comparison among different module types.

ELECTRICAL PARAMETERS AT NOCT

TYPE	JAM72S30 -525/MR	JAM72S30 -530/MR	JAM72S30 -535/MR	JAM72S30 -540/MR	JAM72S30 -545/MR	JAM72S30 -550/MR
Rated Max Power(Pmax) [W]	397	401	405	408	412	416
Open Circuit Voltage(Voc) [V]	46.05	46.18	46.31	46.43	46.55	46.68
Max Power Voltage(Vmp) [V]	38.36	38.57	38.78	38.99	39.20	39.43
Short Circuit Current(Isc) [A]	10.97	11.01	11.05	11.09	11.13	11.17
Max Power Current(Imp) [A]	10.35	10.39	10.43	10.47	10.51	10.55
NOCT	Irradiance 800W/m², ambient temperature 20°C,wind speed 1m/s, AM1.5G					

OPERATING CONDITIONS

Maximum System Voltage	1000V/1500V DC
Operating Temperature	-40℃~+85℃
Maximum Series Fuse Rating	25A
Maximum Static Load,Front* Maximum Static Load,Back*	5400Pa(112lb/ft²) 2400Pa(50lb/ft²)
NOCT	45±2℃
Safety Class	Class Ⅱ
Fire Performance	UL Type 1

CHARACTERISTICS

Current-Voltage Curve JAM72S30-540/MR

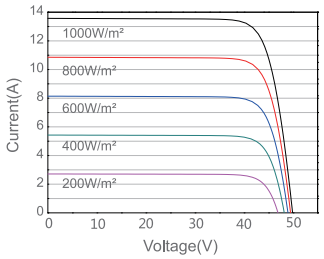

Power-Voltage Curve JAM72S30-540/MR

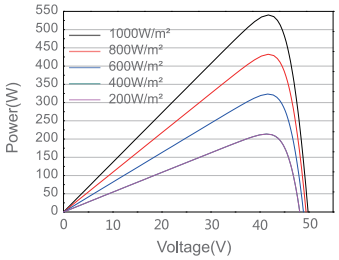

Current-Voltage Curve JAM72S30-540/MR

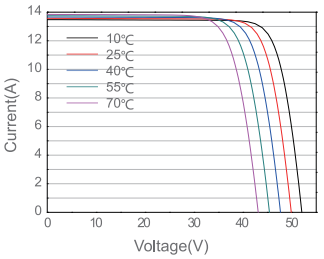

A.1.3 Inverter Datasheet

SUNNY HIGHPOWER PEAK3

Efficient

- High power density with 150 kW thanks to its compact structure
- Max. yield due to possible DC/AC ratio of up to 150%

Reliable

- Superior PV system availability with 150 kW units
- Innovative digital features aligned with the energy management platform ennexOS

Flexible

- For DC input voltages up to 1500 V
- Flexible DC solutions with customer-specific PV array junction boxes

Easy to install

- Ergonomic handling and simple connection for quick installation
- Centralized commissioning and control of the PV power plant via SMA Data Manager

SUNNY HIGHPOWER PEAK3

Customized for tomorrow today

The Sunny Highpower PEAK3 is the central component of the SMA solution for PV power plants with a decentralized architecture and system voltages of 1500 V DC. This compact string inverter enables cost-optimized solutions for industrial PV applications thanks to its high power density. It also provides a simple way of transport and allows for quick installation and commissioning. This string inverter with 150 kW of power is equipped with the automatic SMA Smart Connected service for proactive servicing that facilitates operation and maintenance and reduces service costs throughout the entire project lifetime.

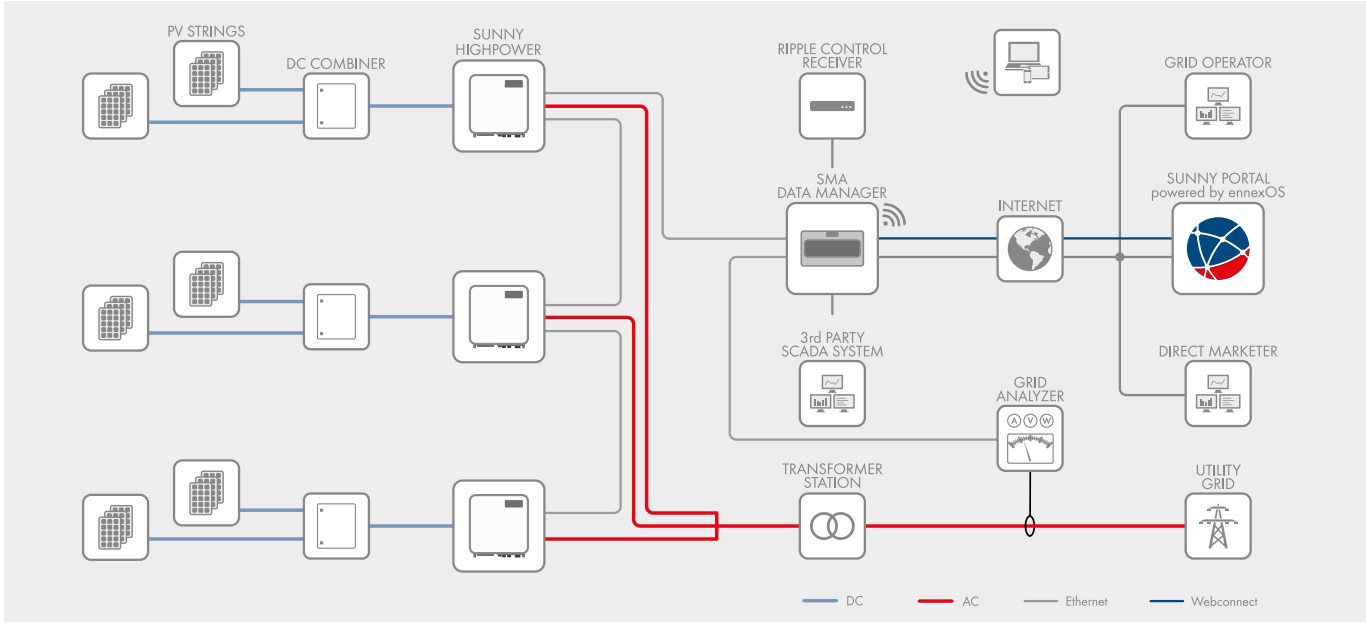

Technical Data	Sunny Highpower 100-20	Sunny Highpower 150-20
Input (DC)		
Max. PV array power	150000 Wp	225000 Wp
Max. input voltage	1000 V	1500 V
MPP voltage range / rated input voltage	590 V to 1000 V / 590 V	880 V to 1450 V / 880 V
Max. input current / max. short-circuit current	180 A / 325 A	180 A / 325 A
Number of independent MPP trackers	1	1
Number of inputs	1 or 2 (optional) for external PV array junction boxes	
Output (AC)		
Rated power at nominal voltage	100000 W	150000 W
Max. apparent power	100000 VA	150000 VA
Nominal AC voltage / AC voltage range	400 V / 304 V to 477 V	600 V / 480 V to 690 V
AC grid frequency / range	50 Hz / 44 Hz to 55 Hz 60 Hz / 54 Hz to 66 Hz	50 Hz / 44 Hz to 55 Hz 60 Hz / 54 Hz to 66 Hz
Rated grid frequency	50 Hz	50 Hz
Max. output current	151 A	151 A
Power factor at rated power / displacement power factor adjustable	1 / 0 overexcited to 0 underexcited	
Harmonic (THD)	< 3%	< 3%
Feed-in phases / AC connection	3 / 3-PE	3 / 3-PE
Efficiency		
Max. efficiency / European efficiency	98.8% / 98.6%	99.1% / 98.8%
Protective devices		
Ground fault monitoring / grid monitoring / DC reverse polarity protection	● / ● / ●	● / ● / ●
AC short-circuit current capability / galvanically isolated	● / –	● / –
All-pole-sensitive residual-current monitoring unit	●	●
Monitored surge arrester (type II) AC / DC	● / ●	● / ●
Protection class (according to IEC 62109-1) / overvoltage category (as per IEC 62109-1)	I / AC: III; DC: II	I / AC: III; DC: II
General Data		
Dimensions (W / H / D)	770 mm / 830 mm / 444 mm (30.3 in / 32.7 in / 17.5 in)	
Weight	98 kg (216 lbs)	
Operating temperature range	-25°C to +60°C (-13°F to +140°F)	
Noise emission (typical)	< 65 dB(A)	
Self-consumption (at night)	< 5 W	
Topology	transformerless	
Cooling method	OptiCool, active cooling, speed-controlled fan	
Degree of protection (according to IEC 60529)	IP65	
Max. permissible value for relative humidity (non-condensing)	100 %	
Features / function / accessories		
DC connection / AC connection	Terminal lug (up to 300 mm²) / Screw terminal (up to 150 mm²)	
LED display (Status / Fault / Communication)	●	
Ethernet interface	● (2 ports)	
Data interface: SMA Modbus / SunSpec Modbus / Speedwire, Webconnect	● / ● / ●	
Mounting type	Rack mounting	
OptiTrac Global Peak / Integrated Plant Control / Q on Demand 24/7	● / ● / ●	
Off-grid capable / SMA Fuel Save Controller compatible	● / ●	
Warranty: 5 / 10 / 15 / 20 years	● / ○ / ○ / ○	
Certificates and approvals (planned)	IEC 62109-1/-2, AR N-4110, AR N-4120, CEI 0-16, C10/11:2012, EN 50549, PEA 2017, DEWA	
● Standard features ○ Optional features – Not available Data at nominal conditions Status: 12/ 2018		
Type designation	SHP 100-20	SHP 150-20

A.1.4 Tracker System Datasheet

GENERAL MECHANICAL **FEATURES**

Tracking type	Horizontal single axis tracker
Typical tracker size	Up to 260 m length
Ground cover ratio (GCR)	Configurable: typical 30-50 %
Wind protection	Zero degree stow position
Corrosion protection	Galvanized steel C3 as standard C4 or C5 on request
Foundation	Sigma
Tracking range	55° as standard Up to 60° upon request
Ground Clearance	300 mm as standard Up to 500 mm on request
Inclination	Up to 36 %
Cleaning	Verified by IDEEMATEC

POWER AND CONTROL **SYSTEM**

Software	Aurora™ by IDEEMATEC
Solar Tracking Method	Astronomical Algorithm 3D adaptive back-tracking
Communication	Full wired redundant data transfer & control flow through power cables, eliminating need for additional cables Reduces the need for trenches, providing cost benefit Wireless communication for self-powered solution
Control	One cluster control unit per 24 MW (250 trackers) – includes weather station, redundancy computer, SCADA ready One motor per tracker control unit
Power	AC power and self-powered solutions UPS available on request
Drive type	High accuracy slew gear – disconnected
Motor type	AC CE 400 V 50 Hz UL 480 V 60 Hz DC 24 V
Operating temperature	-20°C up to +55°C
Warranty	15-years System Warranty

GERMANY / Headquarters
germany@ideematec.com

SPAIN
spain@ideematec.com

FRANCE
france@ideematec.com

PORTUGAL
portugal@ideematec.com

USA
usa@ideematec.com

AUSTRALIA
australia@ideematec.com

CHINA
china@ideematec.com

MENA
mena@ideematec.com

COLOMBIA
colombia@ideematec.com

BRAZIL
brazil@ideematec.com

CHILE
chile@ideematec.com

MEXICO
mexico@ideematec.com

THE COMPLETE TRACKER PORTFOLIO

HORIZON L:TEC® 1P

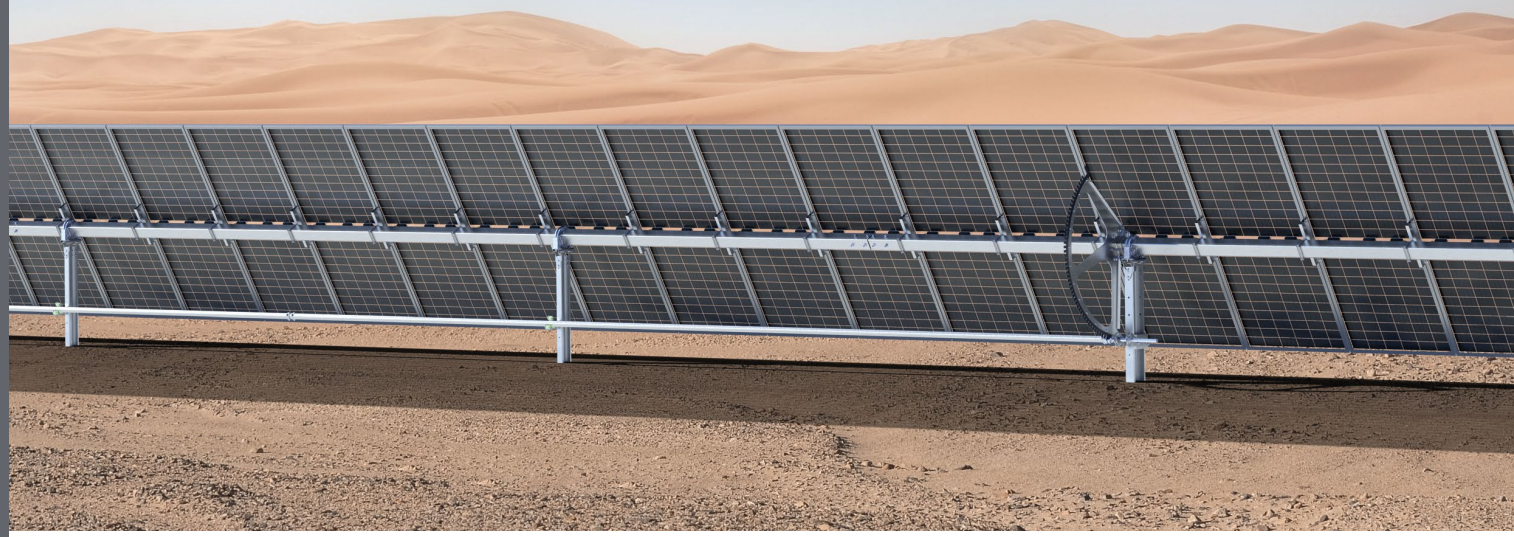

www.ideematec.com

IDEEMATEC

HORIZON L:TEC®

Most advanced **one-in-portrait tracker solution**

The Horizon L:TEC® 1P tracker pairs our signature decoupled drive technology with the new innovative locking system for maximum stability. Designed especially for large modules.

The Horizon L:TEC® is now available in both a one-in-portrait and a two-in-portrait option.

15-YEAR WARRANTY
NEW INDUSTRY BENCHMARK

PATENTED LOCKING AND **DECOUPLED DRIVE TECHNOLOGY**

The decoupled drive technology is significantly more efficient than all traditional drives. The smart drive technology transfers the table loads directly into the foundations and ensures that forces on the drive are kept to an absolute minimum.

This is why we can build the longest and most flexible trackers on the market.

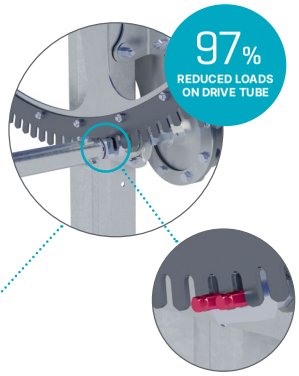

POWERED BY **JUST 1 DRIVE UNIT**

- **3 times less** drive units
- **Higher** availability
- **Lower** maintanance costs

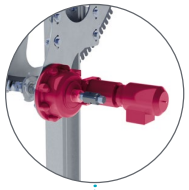

BEST LIFETIME VALUE AND OPTIMIZED LCOE

- **Highest** additional gains
- **Optimizes** overall yields
- **Improves** system lifetime

UP TO **240** MODULES PER TRACKER

UP TO **8** STRINGS PER TRACKER

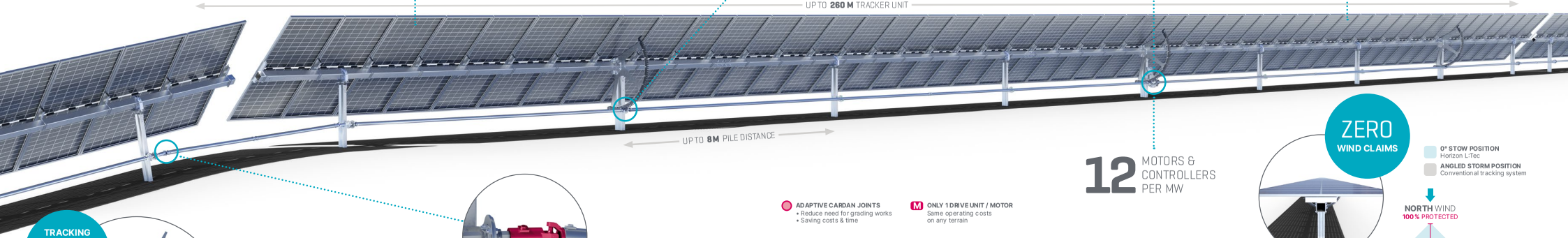

12 MOTORS & CONTROLLERS PER MW

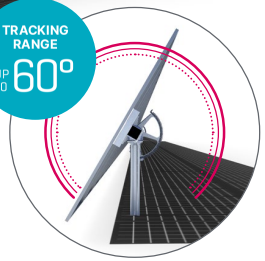

MAXIMUM DESIGN FLEXIBILITY UNLIKE ANY OTHER TRACKER

- **Suits all modules types:** 72 Cells, 78 Cells, bifacial
- **BOS** optimized layout
- **Modular** tracker configuration

PATENTED CARDAN JOINTS **ADAPT TO ANY TERRAIN**

- Each table can be installed at an angle of **up to 36 %** from the previous table
- **No need** for complex grading works

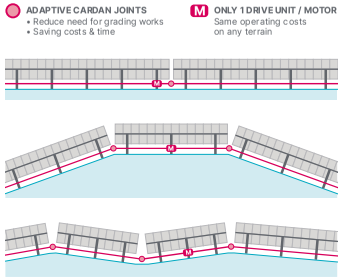

0° STOW POSITION FOR **360° WIND PROTECTION**

- **Unique protection** against extreme weather conditions
- **50 %** less stress with 0° stow
- Withstands winds of **up to 180 km/h**
- **Higher energy** during stowing
- Time-to-stow **max. 6 minutes**

ZERO WIND CLAIMS

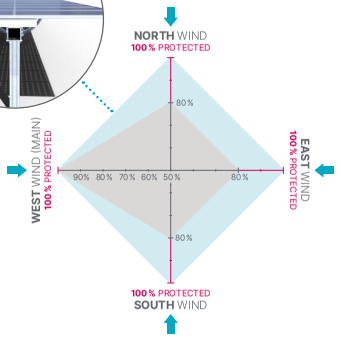

A.2 Ethical Clearance

ETHICAL CLEARANCE CERTIFICATE

Ethical Clearance Reference Number: SOS-0174 Date: 27 OCTOBER 2023

This Ethical Clearance Certificate is issued by the University of Namibia Ethics Committee (REC) in accordance with the University of Namibia's Research Ethics Policy and Guidelines. Ethical approval is given in respect of undertakings contained in the Research Project outlined below. This Certificate is issued on the recommendations of the ethical evaluation done by the ethics committee.

Title of Project: MODELLING AND ANALYSIS OF A PHOTOVOLTAIC SYSTEM FOR A LOCAL BUSINESS IN WINDHOEK, NAMIBIA

Student: AINA KAULUMA

Student Number: 201604520

Supervisor(s): Dr. PETJA DOBREVA

Centre for Research Services

Take note of the following:

1. Any significant changes in the conditions or undertakings outlined in the approved Proposal must be communicated to the ethics committee. An application to make amendments may be necessary.
2. Any breaches of ethical undertakings or practices that have an impact on ethical conduct of the research must be reported to the ethics committee.
3. The Principal Researcher must report issues of ethical compliance to the ethics committee (through the Chairperson) at the end of the Project or as may be requested by the ethics committee.
4. The ethics committee retains the right to:

i) Withdraw or amend this Ethical Clearance if any unethical practices (as outlined in the Research Ethics Policy) have been detected or suspected,

ii) Request for an ethical compliance report at any point during the course of the research.

The ethics committee wishes you the best in your research.

Dr. Zivayi Chiguvare (Chairperson Ethics Committee)

Prof. Davis Mumbengegwi (Head, Multidisciplinary Research)